Continuum Mech. Thermodyn. (2025) 37:28
https://doi.org/10.1007/s00161-024-01356-7

ORIGINAL ARTICLE

N. Challamel · C. Combescure · V. Picandet · M. Ferretti · A. Luongo

Exact bifurcation analysis of the static response of a Fermi–Pasta–Ulam softening chain with short and long-range interactions

Received: 5 December 2023 / Accepted: 25 December 2024 / Published online: 31 January 2025

Abstract This paper is devoted to the static bifurcation of a nonlinear elastic chain with softening and both direct and indirect interactions. This system is also known as a generalized softening FPU system (Fermi–Pasta–lam nonlinear lattice) with $p = 2$ nonlinear interactions (nonlinear direct and second-neighbouring interactions). The static response of this n-degree-of-freedom nonlinear system under pure tension loading is theoretically and numerically investigated. The mathematical problem is equivalent to a nonlinear fourth-order difference eigenvalue problem. The bifurcation parameters are calculated from the exact resolution of the fourth-order linearized difference eigenvalue problem. It is shown that the bifurcation diagram of the generalized softening FPU system depends on the stiffness ratio of both the linear and the nonlinear parts of the nonlinear lattice, which accounts for both short range and long range interactions. This system possesses both a saddle node bifurcation (limit point) and some unstable bifurcation branches for the parameters of interest. We show that for some range of structural parameters, the bifurcations in $(n-1)$ unstable bifurcation branches prevail before the limit point. In the complementary domain of the structural parameters, the bifurcations in $(n-1)$ unstable bifurcation branches prevail after the limit point, which means that the system becomes unstable first, at the limit point. At the border between both domains in the space of structural parameters, the bifurcation in $(n-1)$ unstable bifurcation branches coincide with the limit point, with an addition unstable fundamental branch. This case is the hill-top bifurcation, already analysed by Challamel et al. (Int J Non-Linear Mech 156(104509): 1-11, 2023) in the case $p = 1$ interaction. We also numerically highlight the possibility for such a generalized FPU system to possess possible imperfection sensitivity. Numerical results support the fact that the structural boundary of the hill-top bifurcation coincides with the transition between imperfection sensitive to imperfection insensitive systems.

N. Challamel (✉) · C. Combescure · V. Picandet
IRDL (CNRS UMR 6027), Centre de Recherche, Université Bretagne Sud, Rue de Saint Maudé, BP92116, 56321 Lorient Cedex, France.
E-mail: noel.challamel@univ-ubs.fr

C. Combescure
E-mail: christelle.combescure@univ-ubs.fr

V. Picandet
E-mail: vincent.picandet@univ-ubs.fr

M. Ferretti · A. Luongo
Department of Civil, Construction-Architectural and Environmental Engineering, University of L'Aquila, 67100 L'Aquila, Italy.
E-mail: manuel.ferretti@univaq.it

A. Luongo
E-mail: angelo.luongo@univaq.it

C. Combescure
Saint-Cyr Coëtquidan Military Academy, CReC Saint-Cyr, Guer 56380, France

Keywords Lattice · Nonlinear difference equations · Static bifurcation · Buckling · Stability · Limit point · Saddle-node bifurcation · Nonlinear elasticity · Gradient elasticity · Discrete elasticity

1 Introduction

The exact characterization of finite lattices composed of periodic elements was first elaborated by Lagrange [19] for the vibration of fixed-fixed lattice string or one-dimensional elastic lattice (see also [20]). Lagrange exactly solved a linear second-order difference equation for this associated linear problem, based on only direct interactions (also labelled interactions with the first neighbours). The derivation of an exact solution for a similar vibration problem with generalized interactions with direct and indirect interactions was obtained by Eaton and Peddieson [10] for a generalized fixed-fixed lattice. Eaton and Peddieson [10] implicitly solved a linear $2p$-th order difference equation for a lattice, which includes symmetrical p interactions. The solution of Lagrange was found as a particular case in case of $p = 1$ interaction (only direct interaction with the first neighbours). This $2p$-th order difference equation is associated to $2p$ boundary conditions which may be expressed in difference form with symmetrical arguments (see Challamel et al., [4]). It has been also shown in Challamel et al. [5] that the difference eigenvalue problem is sensitive to the choice of these higher-order boundary conditions ($2p$-2 higher-order boundary conditions expressed in difference form). Drastic change of scale-dependence of the solution may be obtained by modifying these higher-order boundary conditions. The static response of axial lattices with linear direct and indirect interactions has been also studied in the literature. Exact solutions of axial lattice with direct and indirect neighbouring interactions have been obtained in statics, by Toupin and Gazis [25] or Gazis and Wallis [15] from the resolution of a fourth-order linear difference equation for the case $p = 2$ linear interactions. Mindlin [22] also included the influence of a third neighbouring interaction $p = 3$ and solved a 6^{th} order linear difference equation. In particular, Toupin and Gazis [25] discussed the effect of the loading system at the end boundary conditions, and they pointed out the existence of a boundary layer for this problem, and the possible coupling exponential regime for the displacement with a change of sign from one particle to the next. Exact solutions in case of $p = 2$ linear elastic interactions have been derived by Charlotte and Truskinovsky [8] for the static response of such linear lattice ($p = 2$) under pure tension load, with several end boundary conditions. Challamel and Picandet [6] recently reconsidered the static response of such a linear elastic lattice and observed also the change of the solution for the system with different choices of higher-order boundary conditions. The homogeneous solution under pure tension in presence of anti-symmetrical higher-order boundary conditions is changed into an oscillating response for truncated higher-order boundary conditions.

The understanding of nonlinear lattices, both in statics and in dynamics is much more recent, as compared to the initial work of Lagrange restricted to linear systems, and dates from the XX th century. The nonlinear lattice problem is more difficult to handle, due to the lack of theoretical results, in general, in the field of nonlinear difference equations. Fermi, Pasta and Ulam [14] numerically studied the dynamic behaviour of several nonlinear lattices including lattices with polynomial restoring forces (with parabolic and cubic nonlinear terms). Due to this pioneer numerical study on nonlinear lattices, the nonlinear chain is often referred in the literature to the FPU system. The static behaviour of a generalized FPU lattice with polynomial restoring force (up to a 5th order) also including p nonlinear long range interactions has been numerically studied by Triantafyllidis and Bardenhagen [26]. Triantafyllidis and Bardenhagen [26] numerically observed for a FPU system with $p = 2$ interactions (with a polynomial restoring force up to the 5th order) a cascade of very close bifurcation points for this discrete system, close to the limit point in the load–displacement diagram. They also questioned the possibility to approximate this nonlinear lattice problem with a gradient elasticity solution derived by continualization of the initial difference equation (nonlinear difference equation of order $2p$ for the $2p$ interaction problem). Such a continualization of the difference equations of a generalized FPU system with some additional gradient elasticity terms was already achieved by Rosenau [24] in the dynamic context. Truskinovsky and Vainchstein [27] theoretically investigated the stability of the homogeneous strain state of an infinite chain of particles with nonlinear interactions based on Morse potential, and with $p = 2$ or $p = 3$ interactions. They distinguished the instability modes, namely a long wave instability mode (which coincides with the limit point) and a microscopic commensurate instability mode for the infinite chain. Combescure [9] also studied the stability of the homogeneous strain state of an infinite FPU chain with $p = 2$ or $p = 3$ nonlinear interactions of polynomial type (with quintic potential energy), as also considered by Triantafyllidis and Bardenhagen [26]. The stability criteria derived by Truskinovsky and Vainchstein [27] for the infinite chain are confirmed and specified for the specific quintic polynomial interaction. The combination of linear and nonlinear stiffness parameters required to induce either long wave or short-wave instability on the principal path,

have been established. Combescure [9] also numerically studied the response of the finite FPU chain under pure tension load, and explored the possibility to approximate the response of the discrete medium including the bifurcated branches, with either a continuum gradient elasticity or a continuum micromorphic model. Most of the studies to investigate the stability of the post-bifurcated branches are numerical studies based on the definite positiveness of the tangent stiffness matrix according to Lagrange-Dirichlet criterion. Puglisi and Truskinovsky (2000) presented an exhaustive bifurcation diagram for a FPU-type system with initial negative tangent stiffness at the origin. They derived the stability conditions for a nonlinear chain composed of piecewise linear or cubic-type interactions, with $p = 1$ interaction. Challamel et al., [7] reconsidered the finite FPU chain with a cubic-type FPU interaction with initial positive tangent stiffness at the origin, with $p = 1$. They showed that the system is stable until a limit point which coincides with a bifurcated point, where the number of branches depends on the number n of links in the lattice. Such a FPU system admits a multi-degenerate hill-top bifurcation. They also showed that all bifurcated branches are initially unstable, without strong imperfection sensitivity. This softening discrete system is also similar to the self-deploying discrete column studied by Friedman et al., [11], composed of a finite number of softening structural cell which may experience snap-back behaviour.

In the present study, we will explore the stability of a finite generalized FPU system with $p = 2$ interactions under pure tension. The bifurcation loads (or critical displacements) of this finite generalized FPU system are analytically calculated from the resolution of the linearized fourth-order difference eigenvalue problem. The capability of a continuous gradient elasticity approach to capture the bifurcation of the discrete problem is also commented. We show that, for some bifurcation branches of the generalized FPU system, the gradient elasticity model may be asymptotically relevant, whereas for some other bifurcations branches, the gradient elasticity continuum model is less efficient. It is numerically observed that this system may possess imperfection sensitivity for some range of structural parameters. The hill-top bifurcation is also observed at the boundary of the structural parameters, which separates imperfection sensitive and imperfection insensitive domains, in the space of structural parameters.

2 Governing difference equations

Starting from the lattice system with $p = 2$ interactions, the total potential energy of the nonlinear elastic lattice with two closest neighbors under pure tension (see Fig. 1) may be written as:

$$\begin{aligned} W = & \sum_{i=0}^{n-1} \frac{k_1}{2} (u_{i+1} - u_i)^2 - \frac{M_1}{4a^2} (u_{i+1} - u_i)^4 + \sum_{i=0}^{n-2} \frac{k_2}{2} (u_{i+2} - u_i)^2 - \frac{M_2}{4a^2} (u_{i+2} - u_i)^4 \\ & + \frac{k_2}{4} (u_1 - u_{-1})^2 - \frac{M_2}{8a^2} (u_1 - u_{-1})^4 + \frac{k_2}{4} (u_{n+1} - u_{n-1})^2 - \frac{M_2}{8a^2} (u_{n+1} - u_{n-1})^4 \\ & + \lambda_1 u_0 + \lambda_2 (u_n - \overline{u_n}) + \lambda_3 (u_1 + u_{-1}) + \lambda_4 (u_{n+1} - 2u_n + u_{n-1}) \end{aligned} \tag{1}$$

with the following parameter constraints $k_1 \geq 0$, $k_2 \geq 0$ so as to ensure the definite positiveness of the potential energy around the unloaded equilibrium position. We also assume that $M_1 \geq 0$ and $M_2 \geq 0$ (as a generalization of the FPU system considered by Challamel et al., [7] with only $p = 1$ interaction). (k_1, k_2) are the linear stiffness parameters of the first neighbour interaction and the second neighbour interaction, whereas (M_1, M_2) are the nonlinear elasticity parameters of the first neighbour interaction and the second neighbour interaction. $a$is the lattice spacing. The model is constrained by four kinematic constraints, associated to four Lagrange multipliers $(\lambda_1, \lambda_2, \lambda_3, \lambda_4)$:

$$u_0 = 0; \quad u_n = \overline{u_n}; \quad u_{-1} = -u_1 \text{ and } u_{n+1} = 2\overline{u_n} - u_{n-1} \tag{2}$$

It is possible to reexpress the total potential energy by removing the virtual nodes outside the domain which contribute to the higher-boundary conditions, using the two higher-order boundary conditions:

$$u_{-1} = -u_1 \text{ and } u_{n+1} = 2\overline{u_n} - u_{n-1} \tag{3}$$

which gives the equivalent potential, now reduced to two kinematic constraints:

$$W = \sum_{i=0}^{n-1} \frac{k_1}{2} (u_{i+1} - u_i)^2 - \frac{M_1}{4a^2} (u_{i+1} - u_i)^4 + \sum_{i=0}^{n-2} \frac{k_2}{2} (u_{i+2} - u_i)^2 - \frac{M_2}{4a^2} (u_{i+2} - u_i)^4$$
$$+\frac{1}{2} (2k_2) u_1^2 - \frac{(8M_2)}{4a^2} u_1^4 + \frac{1}{2} (2k_2) (u_n - u_{n-1})^2 - \frac{(8M_2)}{4a^2} (u_n - u_{n-1})^4$$
$$+\lambda_1 u_0 + \lambda_2 (u_n - \overline{u_n}) \tag{4}$$

As highlighted on Fig. 1, the lattice is purely periodic except at the border, where stiffness of the second-neighbour interactions has been calibrated with a stiffness of $2k_2$ for the linear part and a term $8M_2$ for the nonlinear one. The calibration of the stiffness at the border, twice the one inside the lattice, in the linear range, has been already commented by Challamel et al., [4] and Challamel et al., [5] for the vibration analysis of a generalized Lagrange lattice, and by Challamel and Picandet [6] in the static regime, in order to fulfill the requirement of the homogeneous response in pure tension (with $p = 2$ interactions). It has also been noted in Combescure [9] for the chain of non-linear springs with $p = 2$ or $p = 3$ interactions, using energy arguments. Such a stiffness calibration is similar to the one considered for calibrating the rotational stiffness of a lattice composed of rigid bars connected by rotational springs (known as Hencky-bar-chain model), where a clamped boundary condition of the Hencky system is associated with an equivalent stiffness twice the one inside the lattice (Hencky in [17] already mentioned this specific calibration of the stiffness at the border of the beam lattice for a clamped boundary condition, as also commented by Challamel et al., [3]). Equation (2) can be also written without kinematic constraints as:

$$W = \sum_{i=1}^{n-2} \frac{k_1}{2} (u_{i+1} - u_i)^2 - \frac{M_1}{4a^2} (u_{i+1} - u_i)^4 + \sum_{i=1}^{n-3} \frac{k_2}{2} (u_{i+2} - u_i)^2 - \frac{M_2}{4a^2} (u_{i+2} - u_i)^4$$
$$+\frac{1}{2} (k_1 + 2k_2) u_1^2 - \frac{(M_1 + 8M_2)}{4a^2} u_1^4 + \frac{1}{2} k_2 u_2^2 - \frac{M_2}{4a^2} u_2^4$$
$$+\frac{1}{2} (k_1 + 2k_2) (\overline{u_n} - u_{n-1})^2 - \frac{(M_1 + 8M_2)}{4a^2} (\overline{u_n} - u_{n-1})^4 + \frac{1}{2} k_2 (\overline{u_n} - u_{n-2})^2 - \frac{M_2}{4a^2} (\overline{u_n} - u_{n-2})^4 \tag{5}$$

Equation (5) is the potential energy formulated for a displacement controlled tension loading of the nonlinear FPU chain with $p = 2$ interactions. It is also possible to express this energy for the same chain in pure tension with a loading controlled test:

$$W = \sum_{i=1}^{n-2} \frac{k_1}{2} (u_{i+1} - u_i)^2 - \frac{M_1}{4a^2} (u_{i+1} - u_i)^4 + \sum_{i=1}^{n-3} \frac{k_2}{2} (u_{i+2} - u_i)^2 - \frac{M_2}{4a^2} (u_{i+2} - u_i)^4$$
$$+\frac{1}{2} (k_1 + 2k_2) u_1^2 - \frac{(M_1 + 8M_2)}{4a^2} u_1^4 + \frac{1}{2} k_2 u_2^2 - \frac{M_2}{4a^2} u_2^4$$
$$+\frac{1}{2} (k_1 + 2k_2) (u_n - u_{n-1})^2 - \frac{(M_1 + 8M_2)}{4a^2} (u_n - u_{n-1})^4 + \frac{1}{2} k_2 (u_n - u_{n-2})^2 - \frac{M_2}{4a^2} (u_n - u_{n-2})^4$$
$$-F u_n \tag{6}$$

The governing equation of this nonlinear lattice is obtained by stationarity of the total potential energy Eq. (1) $\delta W = 0$, thus leading to a fourth-order nonlinear difference equation:

$$k_1 (u_{i+1} - 2u_i + u_{i-1}) - \frac{M_1}{a^2} \left[(u_{i+1} - u_i)^3 - (u_i - u_{i-1})^3 \right]$$
$$+k_2 (u_{i+2} - 2u_i + u_{i-2}) - \frac{M_2}{a^2} \left[(u_{i+2} - u_i)^3 - (u_i - u_{i-2})^3 \right] = 0 \tag{7}$$

coupled with the four boundary conditions given by Eq. (2). When using a load-controlled test, the natural boundary condition at the free end is formulated as:

$$F = (k_1 + 2k_2) (u_n - u_{n-1}) - \frac{(M_1 + 8M_2)}{a^2} (u_n - u_{n-1})^3 + k_2 (u_n - u_{n-2}) - \frac{M_2}{a^2} (u_n - u_{n-2})^3 \tag{8}$$

We remark that the fourth-order nonlinear difference equation is a balance equation which includes short range and long range interactions:

$$N_i^+ - N_i^- = 0 \text{ with } \left\{ \begin{array}{l} N_i^+ = k_1 \left(u_{i+1} - u_i\right) - \frac{M_1}{a^2} \left(u_{i+1} - u_i\right)^3 + k_2 \left(u_{i+2} - u_i\right) - \frac{M_2}{a^2} \left(u_{i+2} - u_i\right)^3 \\ \quad + k_2 \left(u_{i+1} - u_{i-1}\right) - \frac{M_2}{a^2} \left(u_{i+1} - u_{i-1}\right)^3 \\ N_i^- = -k_1 \left(u_{i-1} - u_i\right) + \frac{M_1}{a^2} \left(u_{i-1} - u_i\right)^3 - k_2 \left(u_{i-2} - u_i\right) + \frac{M_2}{a^2} \left(u_{i-2} - u_i\right)^3 \\ \quad - k_2 \left(u_{i-1} - u_{i+1}\right) + \frac{M_2}{a^2} \left(u_{i-1} - u_{i+1}\right)^3 \end{array} \right. \tag{9}$$

The fourth-order nonlinear difference equation can be integrated (in the difference sense) to give a third-order nonlinear difference equation:

$$\begin{aligned} F = {} & k_1 \left(u_{i+1} - u_i\right) - \frac{M_1}{a^2} \left(u_{i+1} - u_i\right)^3 + k_2 \left(u_{i+2} - u_i\right) - \frac{M_2}{a^2} \left(u_{i+2} - u_i\right)^3 + k_2 \left(u_{i+1} - u_{i-1}\right) \\ & - \frac{M_2}{a^2} \left(u_{i+1} - u_{i-1}\right)^3 \end{aligned} \tag{10}$$

It can be checked that the homogeneous solution (fundamental solution):

$$u_i = \overline{u_n} \frac{i}{n} \tag{11}$$

is solution of the nonlinear fourth-order difference equation Eq. (7) coupled with the four boundary conditions Eq. (2). When injecting this fundamental solution in the nonlinear third-order difference equation Eq. (10) gives the load – displacement response of the fundamental solution:

$$F = \left(k_1 + 4k_2\right) \frac{\overline{u_n}}{n} - \frac{M_1 + 16M_2}{a^2} \left(\frac{\overline{u_n}}{n}\right)^3 \tag{12}$$

which can be presented in dimensionless form:

$$\mu = \tilde{u}_n - \frac{M}{k} \left(\tilde{u}_n^3\right) \text{ with } \left\{ \begin{array}{l} k = k_1 + 4k_2 \\ M = M_1 + 16M_2 \end{array} \right. \text{ and } \left\{ \begin{array}{l} \mu = \frac{F}{k\overline{a}} \\ \tilde{u}_n = \frac{\overline{u_n}}{na} \end{array} \right. \tag{13}$$

k is an equivalent linear stiffness and M is an equivalent nonlinear softening stiffness parameter. As already commented by Challamel et al. [7] for $p = 1$ (with only direct interactions), this fundamental branch has a peak associated to the critical values:

$$\tilde{u}_l = \sqrt{\frac{k}{3M}} \text{ and } \mu_l = \frac{2}{3} \sqrt{\frac{k}{3M}} \tag{14}$$

Challamel et al. [7] have shown for $p = 1$ that the fundamental branch is stable in the hardening regime for $\tilde{u} < \tilde{u}_l$, until the peak at $(\tilde{u} = \tilde{u}_l, \mu = \mu_l)$ which coincides with a hill-top bifurcation with $2^n - 1$ unstable bifurcation branches (restricted to n energetically equivalent unstable states in the bifurcation diagram $(\tilde{u}, \mu)$). This point $(\tilde{u} = \tilde{u}_l, \mu = \mu_l)$ is also a limit point for $p = 2$, which generally does not coincide, as we will see, with a hill-top bifurcation.

We can adopt the following dimensionless parameters:

$$\mu^* = \frac{\mu}{\mu_l} \, ; \, \tilde{u}_n^* = \frac{\tilde{u}_n}{\tilde{u}_l} \tag{15}$$

So that the bifurcation path can be expressed in dimensionless form:

$$\mu^* = \frac{\tilde{u}_n^*}{2} \left[3 - \left(\tilde{u}_n^*\right)^2\right] \tag{16}$$

The meaning of the parameters (k_1, k_2, M_1, M_2) could be better understood from an asymptotic behaviour of the governing difference equation, in order to approximate this fourth-order nonlinear difference equation as a non-linear second-order differential equation. We use a continualization process that involves searching for a continuous function $u\left(x = ai\right) = u_i$ which coincides with u_i at the considered nodes i (this method has

been used by Kruskal and Zabusky, [18] for nonlinear axial lattices with direct neighbor interactions, and then also well developed by Rosenau, [24] or Triantafyllidis and Bardenhagen, [26] – see more recently [1]).

Based on the usual continualization process based on $u\,(x = ai) = u_i$, it is possible to expand the spatial difference operator, for sufficiently smooth displacement fields, by using a Taylor-based expansion:

$$u\,(x \pm a) = \sum_{k=0}^{\infty} \frac{(\pm a)^k}{k\,!} \frac{d^k}{dx^k} u\,(x) = \left[e^{ad/dx}\right] u\,(x) \tag{17}$$

so that Eq. (7) may be approximated up the second order expansion by:

$$a^2\,(k_1 + 4k_2)\,\frac{d^2u}{dx^2} - a^2\,(3M_1 + 48M_2)\,\frac{d^2u}{dx^2}\left(\frac{du}{dx}\right)^2 = 0 \tag{18}$$

Higher-order differential equations may be obtained by expanding the difference operators up to higher orders. Using the equivalent nonlinear stiffness parameters calibrated in Eq. (13), the continuum approximation Eq. (18) can be derived in a single differential form:

$$a^2 \frac{d}{dx}\left[k\frac{du}{dx}\left[1 - \frac{M}{k}\left(\frac{du}{dx}\right)^2\right]\right] = 0 \tag{19}$$

which corresponds to the equilibrium equation of a nonlinear elastic bar with a cubic nonlinear stress–strain law:

$$\sigma\,(\varepsilon) = E\varepsilon\left(1 - \frac{M}{k}\varepsilon^2\right) \text{ with } k = \frac{ES}{a} \text{ and } \varepsilon = \frac{du}{dx} \tag{20}$$

where E is an equivalent Young modulus, ε is an equivalent strain and S is an equivalent cross section area of the equivalent nonlinear elastic bar.

3 An analytical study: $n = 2$ cells and $p = 2$ interactions

In order to better understand the behaviour of the FPU chain composed of $n+1$ nodes with $p = 2$ interactions, we start from the simplest case, i.e. n = 2 and p = 2 interactions. For the case $n = 2$ and $p = 2$, the potential energy is reduced to

$$\begin{aligned} W = {} & \frac{1}{2}\,(k_1 + 2k_2)\,u_1^2 - \frac{(M_1 + 8M_2)}{4a^2}u_1^4 + \frac{1}{2}k_2u_2^2 - \frac{M_2}{4a^2}u_2^4 \\ & + \frac{1}{2}\,(k_1 + 2k_2)\,(u_2 - u_1)^2 - \frac{(M_1 + 8M_2)}{4a^2}\,(u_2 - u_1)^4 - Fu_2 \end{aligned} \tag{21}$$

The governing equation of this nonlinear lattice is obtained by stationarity of the total potential energy Eq. (21) $\delta W = 0$:

$$\begin{cases} (k_1 + 2k_2)\,u_1 - \left(\frac{M_1+8M_2}{a^2}\right)u_1^3 - (k_1 + 2k_2)\,(u_2 - u_1) + \left(\frac{M_1+8M_2}{a^2}\right)(u_2 - u_1)^3 = 0 \\ k_2u_2 - \frac{M_2}{a^2}u_2^3 + (k_1 + 2k_2)\,(u_2 - u_1) - \left(\frac{M_1+8M_2}{a^2}\right)(u_2 - u_1)^3 = F \end{cases} \tag{22}$$

We can adopt the following dimensionless parameters:

$$\mu^* = \frac{\mu}{\mu_l}\,;\, \tilde{u}_1^* = \frac{\tilde{u}_1}{\tilde{u}_l}\,;\, \tilde{u}_2^* = \frac{\tilde{u}_2}{\tilde{u}_l}\,;\, \tilde{u}_{2,c}^* = \frac{\tilde{u}_{2,c}}{\tilde{u}_l};\, \alpha = \frac{k_2}{k_1} \text{ and } \beta = \frac{M_2}{M_1} \tag{23}$$

The first equation Eq. (22) can be also equivalently written:

$$(2u_1 - u_2)\left[(k_1 + 2k_2) - \left(\frac{M_1 + 8M_2}{a^2}\right)\left(u_1^2 - u_1u_2 + u_2^2\right)\right] = 0 \tag{24}$$

The fundamental branch is solution of this system of two coupled nonlinear equations in (u_1, u_2):

$$u_i = \frac{i}{2}u_2 \quad \Rightarrow \quad u_1 = \frac{u_2}{2} \tag{25}$$

The fundamental branch can then be expressed in dimensionless form:

$$\begin{cases} \tilde{u}_1^* = \frac{\tilde{u}_2^*}{2} \\ \mu^* = \frac{\tilde{u}_2^*}{2}\left[3 - \left(\tilde{u}_2^*\right)^2\right] \end{cases} \tag{26}$$

The two other branches intersect the fundamental branch at:

$$\begin{cases} 2u_1 - u_2 = 0 \\ (k_1 + 2k_2) - \left(\frac{M_1+8M_2}{a^2}\right)\left(u_1^2 - u_1u_2 + u_2^2\right) = 0 \end{cases} \tag{27}$$

which gives the following bifurcation point:

$$\begin{cases} \tilde{u}_{1,c}^* = \frac{1}{2}\sqrt{\left(\frac{1+2\alpha}{1+4\alpha}\right)\left(\frac{1+16\beta}{1+8\beta}\right)} \\ \tilde{u}_{2,c}^* = \sqrt{\left(\frac{1+2\alpha}{1+4\alpha}\right)\left(\frac{1+16\beta}{1+8\beta}\right)} \end{cases} \tag{28}$$

The two bifurcation branches are obtained from the resolution of Eqs. (22) and (24):

$$\begin{cases} \tilde{u}_1^* = \frac{\tilde{u}_2^* \pm \sqrt{3\left[\left(\tilde{u}_{2,c}^*\right)^2 - \left(\tilde{u}_2^*\right)^2\right]}}{2} \\ \mu^* = \frac{3\alpha}{1+4\alpha}\tilde{u}_2^* - \frac{4\beta}{1+16\beta}\left(\tilde{u}_2^*\right)^3 + \frac{3(1+2\alpha)}{1+4\alpha}\left(\tilde{u}_2^* - \tilde{u}_1^*\right) - \frac{4(1+8\beta)}{1+16\beta}\left(\tilde{u}_2^* - \tilde{u}_1^*\right)^3 \end{cases} \tag{29}$$

It can be shown easily that:

$$\mu_c^* = \frac{1}{2}\sqrt{\left(\frac{1+2\alpha}{1+4\alpha}\right)\left(\frac{1+16\beta}{1+8\beta}\right)}\left[3 - \left(\frac{1+2\alpha}{1+4\alpha}\right)\left(\frac{1+16\beta}{1+8\beta}\right)\right] < 1 \tag{30}$$

From Eq. (28), we obtain the three cases:

$$\begin{cases} 4\beta < \alpha \quad \Rightarrow \quad \tilde{u}_c^* < 1 \\ 4\beta = \alpha \quad \Rightarrow \quad \tilde{u}_c^* = 1 \\ 4\beta > \alpha \quad \Rightarrow \quad \tilde{u}_c^* > 1 \end{cases} \tag{31}$$

For $4\beta < \alpha$, the bifurcation in two (energetically equivalent) unstable bifurcation branches, prevails before the limit point. For $4\beta = \alpha$, the bifurcation in two (energetically equivalent) unstable bifurcation branches coincides with the limit point, with an addition unstable fundamental branch (*3* unstable bifurcation branches). This case is the hill-top bifurcation, already analysed by Challamel et al. [7] in case $p = 1$ (which includes the case $4\beta = \alpha = 0$). When $4\beta > \alpha$, the bifurcation in two (energetically equivalent) unstable bifurcation branches prevails after the limit point, which means that the system becomes unstable first at the limit point (saddle node bifurcation). The bifurcation diagrams are shown in Figs. 2, 3, 4, 5, 6, 7, 8, 9 and 10. Figures 2, 3 and 4 illustrate the case where the bifurcation prevails before the limit point ($4\beta < \alpha$). Figure 3 shows that the bifurcation path (denoted by *BP*) which precedes the limit point, is a loop. This loop is unstable according to Lagrange–Dirichlet criterion. Figures 5, 6 and 7 show the hill-top bifurcation diagram associated to the limit case $4\beta = \alpha$. The bifurcation path which also forms a loop and starts at the limit point in this case is also unstable according to Lagrange-Dirichlet criterion. Figures 8, 9 or 10 show a typical example of saddle node bifurcation (limit point), followed by the symmetrically unstable bifurcation in two energetically equivalent branches ($4\beta > \alpha$). The bifurcation path is also a loop in the spatial tree-dimensional bifurcation diagram (see Fig. 9).

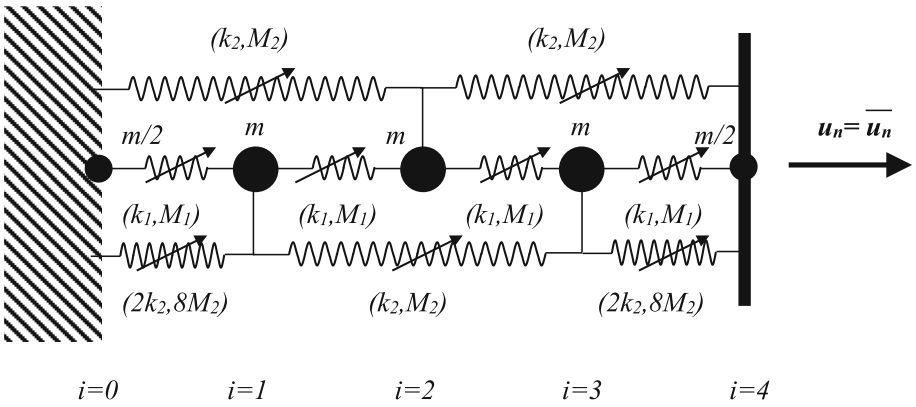

Fig. 1 Tension of a generalized FPU system with $p = 2$ interactions and $n = 4$

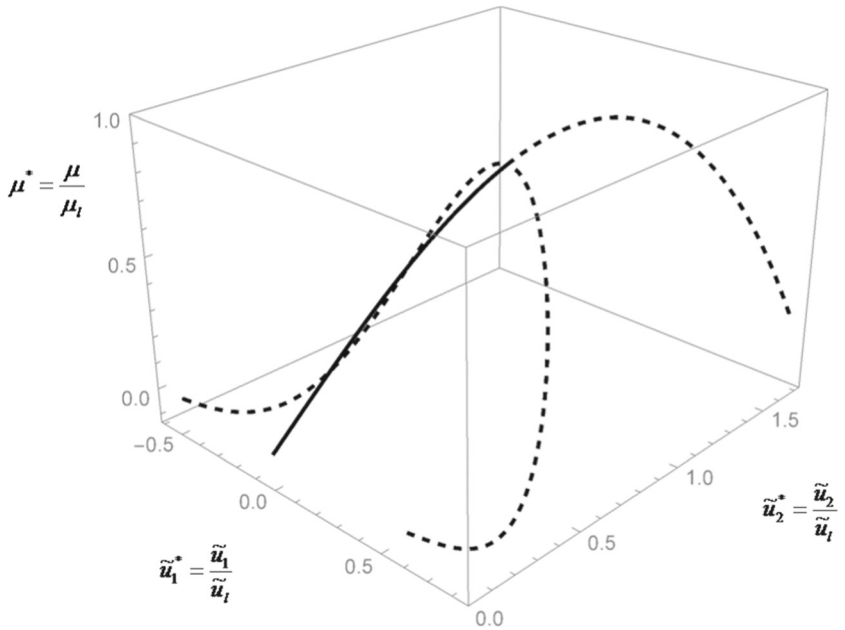

Fig. 2 $n = 2$; $p = 2$; Bifurcation before the limit point; 3D representation of the bifurcation diagram; $\left(\tilde{u}_1^*, \tilde{u}_2^*, \mu^*\right)$; $\alpha = 16$; $\beta = 0$; Case $\alpha > 4\beta$; $\tilde{u}_{2,c}^* = 0.7125 < 1$

The stability of each branch can be easily characterized thanks to Lagrange-Dirichlet criterion. The stiffness matrix is calculated from the second variation of the total potential energy:

$$\begin{cases} K_{11} = 2k_1 + 4k_2 - \frac{3(M_1+8M_2)}{a^2}u_1^2 - \frac{3(M_1+8M_2)}{a^2}(u_2-u_1)^2 \\ K_{12} = K_{21} = -(k_1+2k_2) + \frac{3(M_1+8M_2)}{a^2}(u_2-u_1)^2 \\ K_{22} = k_1 + 3k_2 - \frac{3M_2}{a^2}u_2^2 - \frac{3(M_1+8M_2)}{a^2}(u_2-u_1)^2 \end{cases} \tag{32}$$

which can be presented in dimensionless form thanks to $K_{ij}^* = K_{ij}/k$:

$$\begin{cases} K_{11}^* = \frac{2+4\alpha}{1+4\alpha} - \frac{4(1+8\beta)}{1+16\beta}\left(\tilde{u}_1^*\right)^2 - \frac{4(1+8\beta)}{1+16\beta}\left(\tilde{u}_2^* - \tilde{u}_1^*\right)^2 \\ K_{12}^* = K_{21}^* = -\left(\frac{1+2\alpha}{1+4\alpha}\right) + \frac{4(1+8\beta)}{1+16\beta}\left(\tilde{u}_2^* - \tilde{u}_1^*\right)^2 \\ K_{22}^* = \frac{1+3\alpha}{1+4\alpha} - \frac{4\beta}{1+16\beta}\left(\tilde{u}_2^*\right)^2 - \frac{4(1+8\beta)}{1+16\beta}\left(\tilde{u}_2^* - \tilde{u}_1^*\right)^2 \end{cases} \tag{33}$$

Sylvester's criterion can be used to check the stability of each branch:

$$K_{11}^* > 0 \text{ and } K_{11}^* K_{22}^* - \left(K_{12}^*\right)^2 > 0 \tag{34}$$

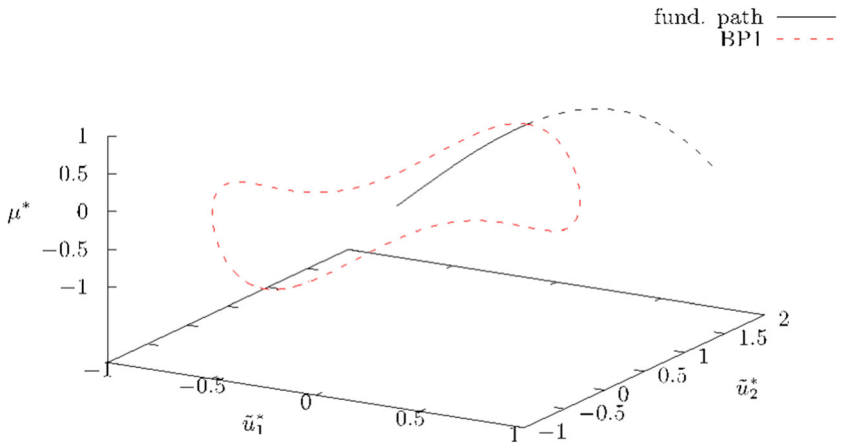

Fig. 3 $n = 2$; $p = 2$; Bifurcation before the limit point; 3D representation of the bifurcation diagram; $\left(\tilde{u}_1^*, \tilde{u}_2^*, \mu^*\right)$; $\alpha = 16$; $\beta = 0$; Case $\alpha > 4\beta$; $\tilde{u}_{2,c}^* = 0.7125 < 1$; The post-bifurcation path is a loop

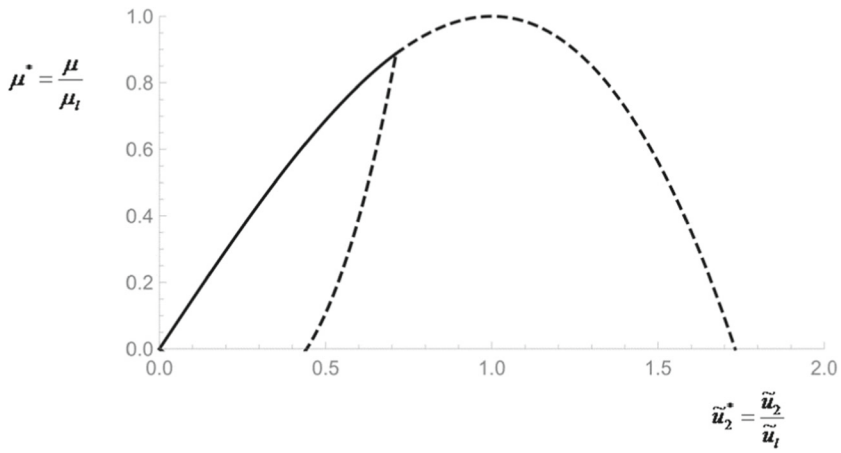

Fig. 4 $n = 2$; $p = 2$; Bifurcation before the limit point; 2D representation of the bifurcation diagram; $\left(\tilde{u}_2^*, \mu^*\right)$; $\alpha = 16$; $\beta = 0$; Case $\alpha > 4\beta$; $\tilde{u}_{2,c}^* = 0.7125 < 1$

For the fundamental branch, we have:

$$\tilde{u}_1^* = \frac{\tilde{u}_2^*}{2} \quad \Rightarrow \quad \begin{cases} K_{11}^* = \frac{2(1+2\alpha)}{1+4\alpha} - \frac{2(1+8\beta)}{1+16\beta}\left(\tilde{u}_2^*\right)^2 \\ K_{12}^* = K_{21}^* = -\left(\frac{1+2\alpha}{1+4\alpha}\right) + \frac{(1+8\beta)}{1+16\beta}\left(\tilde{u}_2^*\right)^2 \\ K_{22}^* = \frac{1+3\alpha}{1+4\alpha} - \frac{1+12\beta}{1+16\beta}\left(\tilde{u}_2^*\right)^2 \end{cases} \tag{35}$$

It can be checked that $K_{11}^* = 0$ vanishes at the bifurcation point $\left(\tilde{u}_1^* = \tilde{u}_{1,c}^*, \tilde{u}_2^* = \tilde{u}_{2,c}^*\right)$, which may be associated to the so-called micro-instability, whereas the global determinant $K_{11}^* K_{22}^* - \left(K_{12}^*\right)^2 = 0$ vanishes at the limit point $\left(\tilde{u}_1^* = 1/2, \tilde{u}_2^* = 1\right)$, which is recognized as the macro-instability. Both are instability phenomena associated to a distinguished bifurcation. For all cases, the bifurcation branches are shown to be unstable, according to Lagrange–Dirichlet instability criterion.

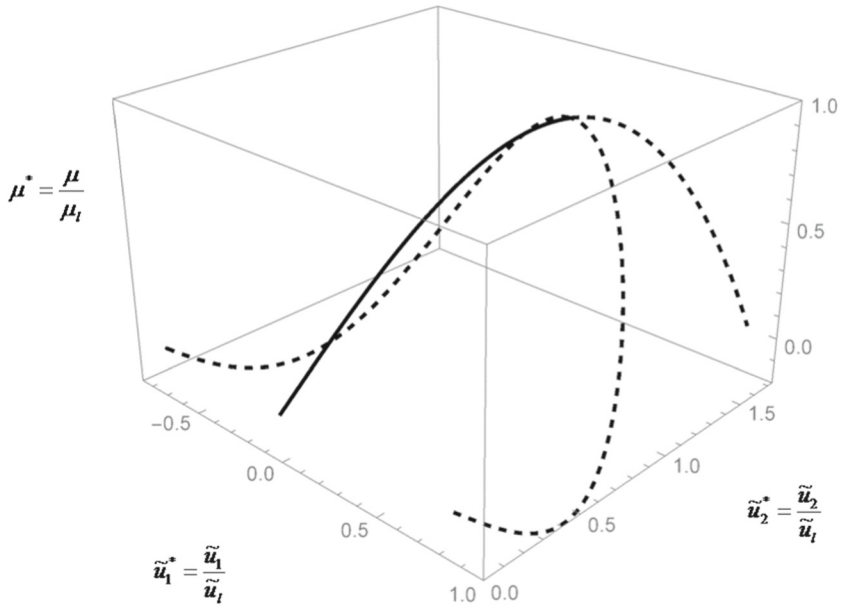

Fig. 5 $n = 2$; $p = 2$; Hill-top bifurcation; 3D representation of the bifurcation diagram; $\left(\tilde{u}_1^*, \tilde{u}_2^*, \mu^*\right)$; $\alpha = 16$; $\beta = 4$; Case $\alpha = 4\beta$; $\tilde{u}_{2,c}^* = 1$

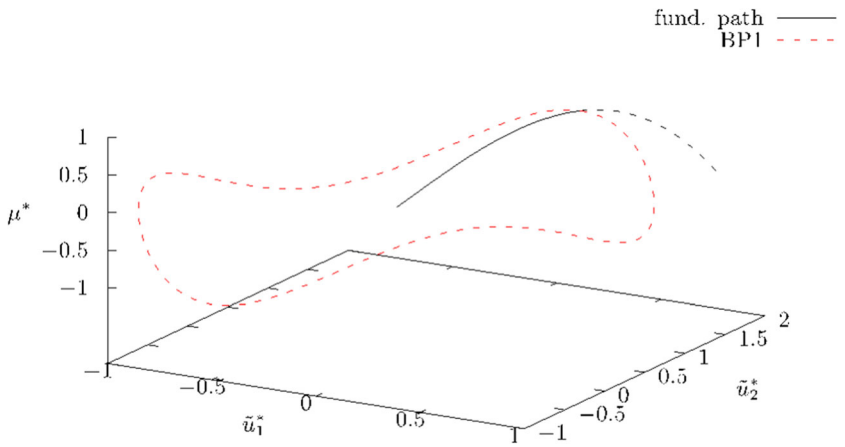

Fig. 6 $n = 2$; $p = 2$; Hill-top bifurcation; 3D representation of the bifurcation diagram; $\left(\tilde{u}_1^*, \tilde{u}_2^*, \mu^*\right)$; $\alpha = 16$; $\beta = 4$; Case $\alpha = 4\beta$; $\tilde{u}_{2,c}^* = 1$; The post-bifurcation path is a loop

4 Results for a general chain of dimension n (with $p = 2$)

In the general case, for $p = 2$, the fourth-order nonlinear difference eigenvalue problem to be solved for general values of n is obtained from:

$$\begin{aligned} &k_1 \left(u_{i+1} - 2u_i + u_{i-1}\right) - \frac{M_1}{a^2}\left[\left(u_{i+1} - u_i\right)^3 - \left(u_i - u_{i-1}\right)^3\right] \\ &+k_2 \left(u_{i+2} - 2u_i + u_{i-2}\right) - \frac{M_2}{a^2}\left[\left(u_{i+2} - u_i\right)^3 - \left(u_i - u_{i-2}\right)^3\right] = 0 \\ &\text{with } u_0 = 0; \quad u_n = \overline{u_n} \quad ; \quad u_{-1} = -u_1 \text{ and } u_{n+1} = 2\overline{u_n} - u_{n-1} \end{aligned} \tag{36}$$

It can be convenient to proceed with the change of variable of the perturbed solution with respect to the fundamental homogeneous solution:

$$v_i = u_i - \overline{u}\frac{i}{n} \tag{37}$$

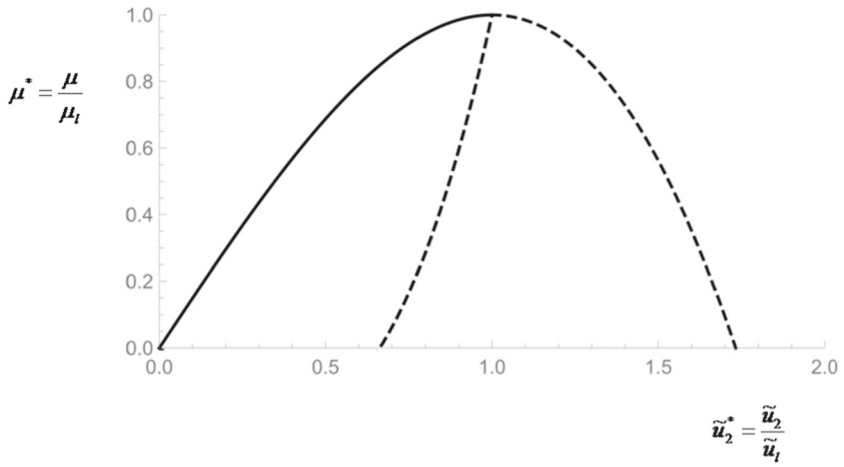

Fig. 7 $n = 2$; $p = 2$; Hill-top bifurcation; 2D representation of the bifurcation diagram; $\left(\tilde{u}_2^*, \mu^*\right)$; $\alpha = 16$; $\beta = 4$; Case $\alpha = 4\beta$; $\tilde{u}_{2,c}^* = 1$

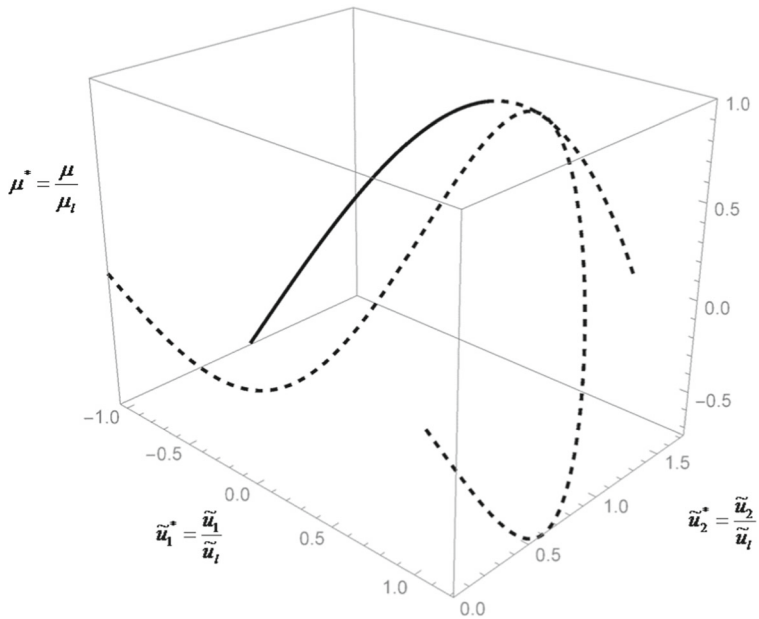

Fig. 8 $n = 2$; $p = 2$; Bifurcation after the limit point; 3D representation of the bifurcation diagram; $\left(\tilde{u}_1^*, \tilde{u}_2^*, \mu^*\right)$; $\alpha = 1/4$; $\beta = 8$; Case $\alpha < 4\beta$; $\tilde{u}_{2,c}^* = 1.2200 > 1$

so that the fourth-order nonlinear difference eigenvalue problem is reformulated with fixed end boundary conditions:

$$
\begin{aligned}
&k_1 \left(v_{i+1} - 2v_i + v_{i-1}\right) - \frac{M_1}{a^2} \left(v_{i+1} - 2v_i + v_{i-1}\right) \\
&\left[\left(v_{i+1} - v_i\right)^2 + \left(v_{i+1} - v_i\right)\left(v_i - v_{i-1}\right) + \left(v_i - v_{i-1}\right)^2 + 3\frac{\bar{u}}{n}\left(v_{i+1} - v_{i-1}\right) \quad + 3\left(\frac{\bar{u}}{n}\right)^2\right] \\
&\quad + k_2 \left(v_{i+2} - 2v_i + v_{i-2}\right) - \frac{M_2}{a^2} \left(v_{i+2} - 2v_i + v_{i-2}\right) \\
&\left[\left(v_{i+2} - v_i\right)^2 + \left(v_{i+2} - v_i\right)\left(v_i - v_{i-2}\right) + \left(v_i - v_{i-2}\right)^2 + 6\frac{\bar{u}}{n}\left(v_{i+2} - v_{i-2}\right) + 12\left(\frac{\bar{u}}{n}\right)^2\right] \\
&= 0 \quad \text{with } v_0 = 0;\ v_n = 0;\ v_{-1} = -v_1 \text{ and } v_{n+1} = -v_{n-1}
\end{aligned}
\tag{38}
$$

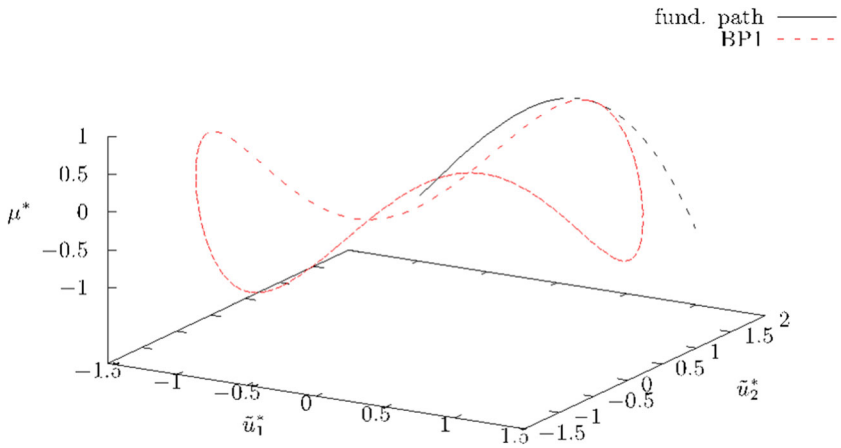

Fig. 9 $n = 2$; $p = 2$; Bifurcation after the limit point; 3D representation of the bifurcation diagram; $\left(\tilde{u}_1^*, \tilde{u}_2^*, \mu^*\right)$; $\alpha = 1/4$; $\beta = 8$; Case $\alpha < 4\beta$; $\tilde{u}_{2,c}^* = 1.2200 > 1$

The linearized fourth-order difference eigenvalue problem will be studied in order to explicitly calculate the bifurcation load (or critical displacement). When only considering the linear terms in the previous difference eigenvalue problem, we obtain the linear fourth-order difference eigenvalue problem:

$$\left[k_1 - 3M_1\left(\frac{\overline{u}}{an}\right)^2\right](v_{i+1} - 2v_i + v_{i-1}) + \left[k_2 - 12M_2\left(\frac{\overline{u}}{an}\right)^2\right](v_{i+2} - 2v_i + v_{i-2}) = 0$$
$$\text{with } v_0 = 0;\ v_n = 0;\ v_{-1} = -v_1 \text{ and } v_{n+1} = -v_{n-1} \tag{39}$$

which can be reformulated using dimensionless quantities:

$$\left[1 - \left(\frac{1+4\alpha}{1+16\beta}\right)\left(\tilde{u}_n^*\right)^2\right](v_{i+1} - 2v_i + v_{i-1}) + \left[\alpha - 4\beta\left(\frac{1+4\alpha}{1+16\beta}\right)\left(\tilde{u}_n^*\right)^2\right](v_{i+2} - 2v_i + v_{i-2}) = 0$$
$$\text{with } v_0 = 0;\ v_n = 0;\ v_{-1} = -v_1 \text{ and } v_{n+1} = -v_{n-1} \tag{40}$$

where we have used, as introduced before, the following parameters:

$$k = k_1 + 4k_2; \quad M = M_1 + 16M_2; \quad \tilde{u}_n = \frac{\overline{u_n}}{na}\ ; \tilde{u}_l = \sqrt{\frac{k}{3M}}; \tilde{u}_n^* = \frac{\tilde{u}_n}{\tilde{u}_l}\ ; \tilde{u}_{n,c}^* = \frac{\tilde{u}_{n,c}}{\tilde{u}_l};$$
$$\alpha = \frac{k_2}{k_1} \text{ and } \beta = \frac{M_2}{M_1} \tag{41}$$

It can be checked easily from the continualization of the linearized fourth-order difference equation in Eq. (40) that the second-order differential equation in the asymptotic limit corresponds to the one associated with the tangent modulus. Using the expansion of the discrete Laplacian based on:

$$v_{i+1} - 2v_i + v_{i-1} = a^2\frac{d^2v}{dx^2} + \mathrm{O}\left(a^4\right) \text{ and } v_{i+2} - 2v_i + v_{i-2} = 4a^2\frac{d^2v}{dx^2} + \mathrm{O}\left(a^4\right) \tag{42}$$

The linear fourth-order difference equation is then approximated in the long wave limit by:

$$a^2\left(1 + 4\alpha\right)\left[1 - \left(\tilde{u}_n^*\right)^2\right]\frac{d^2v}{dx^2} + \mathrm{O}\left(a^4\right) = 0 \tag{43}$$

Equation (43) confirms the existence of the limit point for $\tilde{u}_n^* = 1$. It is possible to rewrite the linear fourth-order difference equation Eq. (40) using some alternative dimensionless parameters γ_1 and γ_2 , in the case $\tilde{u}_n^* \neq 1$ (outside the limit point):

$$\gamma_1\left(v_{i+1} - 2v_i + v_{i-1}\right) + \frac{\gamma_2}{4}\left(v_{i+2} - 2v_i + v_{i-2}\right) = 0 \tag{44}$$

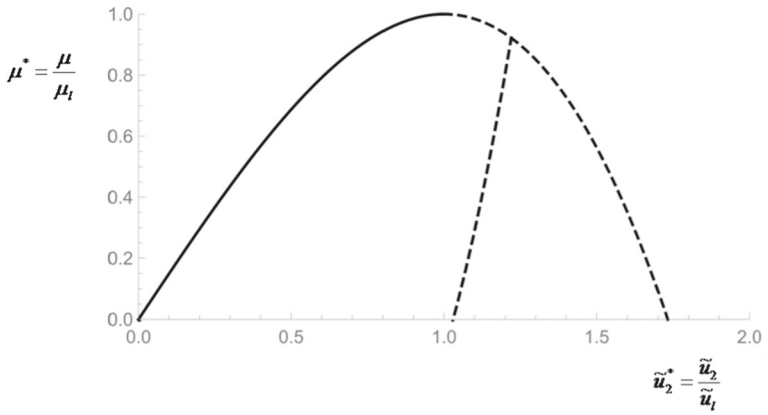

Fig. 10 $n = 2$; $p = 2$; Bifurcation after the limit point; 2D representation of the bifurcation diagram; $\left(\tilde{u}_2^*, \mu^*\right)$; $\alpha = 1/4$; $\beta = 8$; Case $\alpha < 4\beta$; $\tilde{u}_{2,c}^* = 1.2200 > 1$

where the dimensionless parameters affecting each difference operator are identified as:

$$\gamma_1 = \frac{\frac{1}{1+4\alpha} - \frac{\left(\tilde{u}_n^*\right)^2}{1+16\beta}}{1 - \left(\tilde{u}_n^*\right)^2} \text{ and } \gamma_2 = \frac{\frac{4\alpha}{1+4\alpha} - \frac{16\beta\left(\tilde{u}_n^*\right)^2}{1+16\beta}}{1 - \left(\tilde{u}_n^*\right)^2} \tag{45}$$

It can be checked that these two coefficients can be understood as weighting coefficients of the discrete Laplacian operators (second-order difference operator for the one-dimensional investigated in the paper):

$$\gamma_1 + \gamma_2 = 1 \tag{46}$$

This linear fourth-order difference equation Eq. (44) can be equivalently rewritten:

$$v_{i+1} - 2v_i + v_{i-1} + \frac{\gamma_2}{4}\left(v_{i+2} - 4v_{i+1} + 6v_i - 4v_{i-1} + v_{i-2}\right) = 0 \tag{47}$$

which can be presented in a condensed formula:

$$\Delta\left(1 + \frac{a^2\gamma_2}{4}\Delta\right)v_i = 0 \tag{48}$$

where Δ is the discrete Laplacian, i.e. $\Delta v_i = (v_{i+1} - 2v_i + v_{i-1})/a^2$. The linear fourth-order difference equation Eq. (48) is factorized by the discrete Laplacian operator. The other linear second-order difference equation which controls the form of solution is written explicitly:

$$v_i + \frac{\gamma_2}{4}\left(v_{i+1} - 2v_i + v_{i-1}\right) = 0 \tag{49}$$

The solution of this linear second-order difference equation is sought in the form (see Goldberg, [16]; Elaydi, [12]):

$$v_i = \sum_{p\in\{1,2\}} C_p f_p^i \tag{50}$$

where the two solutions of the characteristic equation f_p are detailed below

$$f^2 + \left(\frac{4}{\gamma_2} - 2\right)f + 1 = 0 \tag{51}$$

whose solutions may be expressed by:

$$f_{1,2} = 1 - \frac{2}{\gamma_2} \pm \sqrt{\left(1 - \frac{2}{\gamma_2}\right)^2 - 1} \tag{52}$$

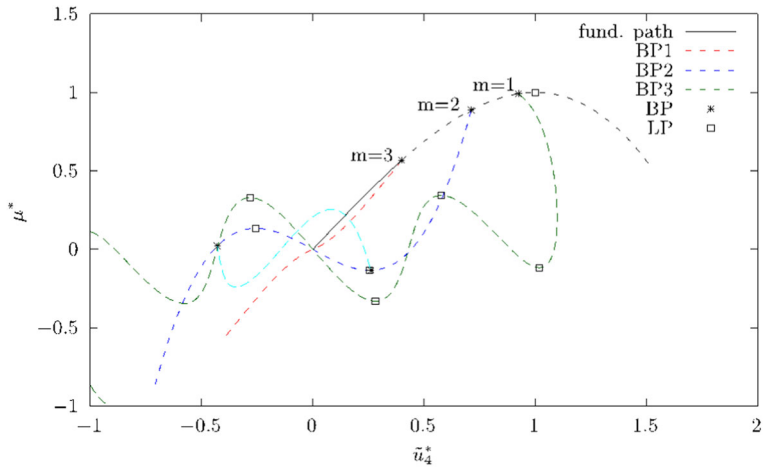

Fig. 11 $n = 4$; $p = 2$; Bifurcations before the limit point LP $\left(\tilde{u}_4^*, \mu^*\right) = (1, 1)$; Bifurcation diagram $\left(\tilde{u}_4^*, \mu^*\right)$; $\alpha = 16$; $\beta = 0$; Case $\alpha > 4\beta$; Bifurcation points $\left(\tilde{u}_{4,c}^*, \mu_c^*, m\right) = (0.3995, 0.5673, 3)$; $\left(\tilde{u}_{4,c}^*, \mu_c^*, m\right) = (0.7125, 0.8879, 2)$; $\left(\tilde{u}_{4,c}^*, \mu_c^*, m\right) = (0.9251, 0.9918, 1)$

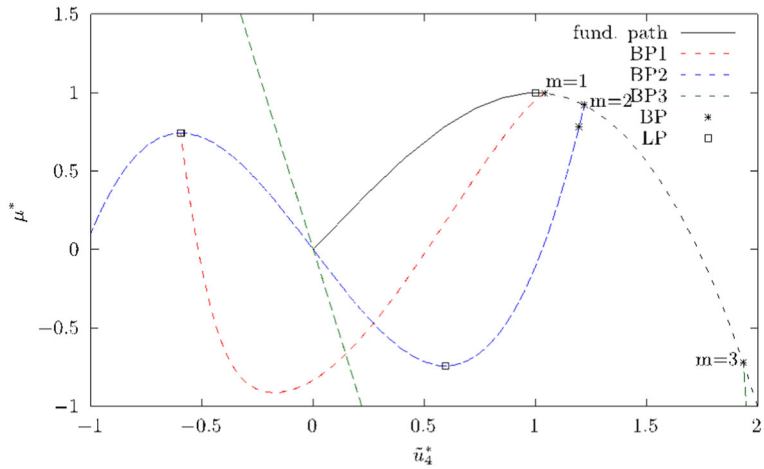

Fig. 12 $n = 4$; $p = 2$; Bifurcations after the limit point LP $\left(\tilde{u}_4^*, \mu^*\right) = (1, 1)$; Bifurcation diagram $\left(\tilde{u}_4^*, \mu^*\right)$; $\alpha = 1/4$; $\beta = 8$; Case $\alpha < 4\beta$; Bifurcation points $\left(\tilde{u}_{4,c}^*, \mu_c^*, m\right) = (1.0413, 0.9974, 1)$; $\left(\tilde{u}_{4,c}^*, \mu_c^*, m\right) = (1.2200, 0.9221, 2)$; $\left(\tilde{u}_{4,c}^*, \mu_c^*, m\right) = (1.9352, -0.7209, 3)$

The form of solution is controlled by the value of γ_2 which depends on the imposed displacement $\tilde{u}_n^*$, which plays the role of the eigenvalue parameter. In the limit of the free unconstrained system $\tilde{u}_n^* = 0$, this critical parameter γ_2 is positive and smaller than unity:

$$\tilde{u}_n^* = 0 \quad \Rightarrow \quad \gamma_2 = \frac{4\alpha}{1+4\alpha} \in [0;\, 1[\quad \Rightarrow \quad 1 - \frac{2}{\gamma_2} < -1 \tag{53}$$

γ_2 is still positive and smaller than unity, for sufficiently small constrained system:

$$\tilde{u}_n^* < \sqrt{\frac{1+16\beta}{1+4\alpha}}, \tilde{u}_n^* < \sqrt{\frac{1+16\beta}{1+4\alpha}}\sqrt{\frac{\alpha}{4\beta}} \text{ and } \tilde{u}_n^* < 1 \quad \Rightarrow \quad \gamma_2 \in [0;\, 1[\quad \Rightarrow \quad 1 - \frac{2}{\gamma_2} < -1 \tag{54}$$

so that the solutions may be equivalently reexpressed by:

$$f_{1,2} = -\cosh\theta \pm \sinh\theta \text{ with } \theta = a\cosh\left(1 + 2\frac{\gamma_1}{\gamma_2}\right) = a\cosh\left(\frac{2}{\gamma_2} - 1\right) \tag{55}$$

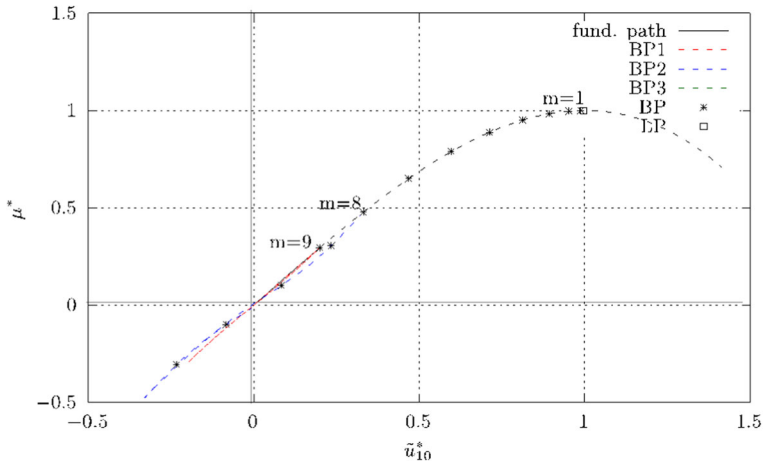

Fig. 13 $n = 10$; $p = 2$; Bifurcations before the limit point LP $\left(\tilde{u}^*_{10}, \mu^*\right) = (1, 1)$; Bifurcation diagram $\left(\tilde{u}^*_{10}, \mu^*\right)$; $\alpha = 16$; $\beta = 0$; Case $\alpha > 4\beta$; First bifurcation point at $\left(\tilde{u}^*_{10,c}, \mu^*_c\right) = (0.198695, 0.29412)$ for $m = 9$

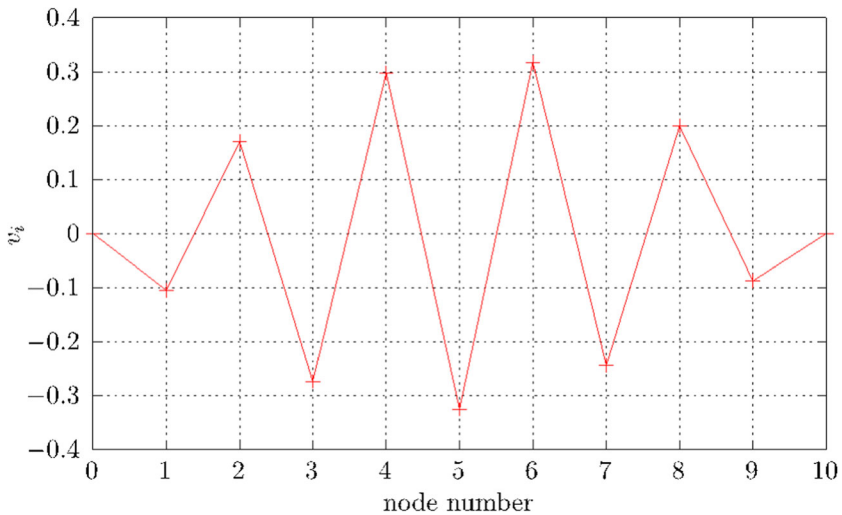

Fig. 14 $n = 10$; $p = 2$; $\alpha = 16$; $\beta = 0$; Case $\alpha > 4\beta$; First bifurcation mode at $\left(\tilde{u}^*_{10}, \mu^*\right) = (0.18805, 0.27662)$ for $m = 9$ close to the first bifurcation point

The solution to Eq. (47) can be finally written as the sum of a linear solution and an exponential one with alternate sign:

$$v_i = A_1 + A_2 i + A_3 (-1)^i \cosh(\theta\, i) + A_{\prime 4} (-1)^i \sinh(\theta\, i) \tag{56}$$

This is in adequacy with the solution derived by Challamel et al. [5] for dynamic problems, when the inertia effects are neglected, or the solution of Challamel and Picandet [6] for the static of a linear chain with $p = 2$ interactions. Toupin and Gazis [25] or Gazis and Wallis [15] already remark for a similar problem (linear lattice with short and long range interactions), that the amplitude of the displacement varies exponentially with the position of the particle, but the sign changes from one particle to the next. It is worth mentioning that Charlotte and Truskinovsky [8] also concluded for such linear lattices (with positive short-range and long-range stiffness parameters) that the boundary layer contains some oscillations at the scale of the lattice modulated by an exponential envelope. Here, we obtain similar results for the linearized nonlinear lattice for sufficiently small displacement constraints. For this range of parameter and considering the four boundary conditions leads to the vanishing perturbed solution (uniqueness of the solution for this range of parameter):

$$A_1 = A_2 = A_3 = A_{\prime 4} = 0 \quad \Rightarrow \quad v_i = 0 \tag{57}$$

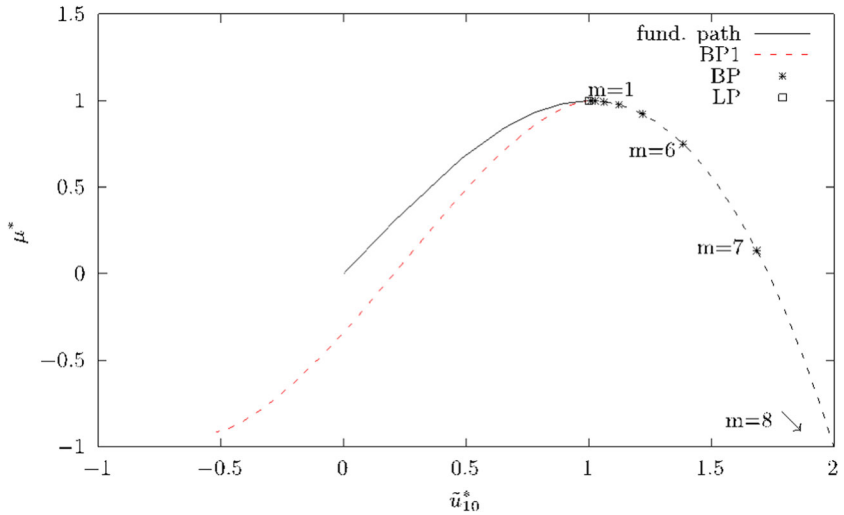

Fig. 15 $n = 10$; $p = 2$; Bifurcations after the limit point $\left(\tilde{u}^*_{10}, \mu^*\right) = (1, 1)$; Bifurcation diagram $\left(\tilde{u}^*_{10}, \mu^*\right)$; $\alpha = 1/4$; $\beta = 8$; Case $\alpha < 4\beta$; First bifurcation point *BP* after the limit point *LP* at $\left(\tilde{u}^*_{10,c}, \mu^*_c\right) = (1.00615, 0.999943)$ for $m = 1$

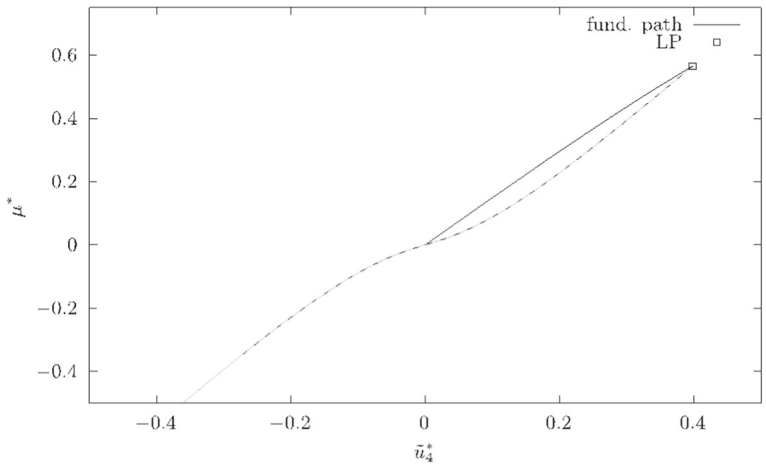

Fig. 16 $n = 4$; $p = 2$; Effect of an imperfection; Imperfection set up on the first non-linear spring of stiffness parameters $(0.99k_1, 0.99M_1)$ between nodes $i = 0$ and $i = 1$; $\alpha = 16$; $\beta = 0$; Case $\alpha > 4\beta$;Limit point *LP* of the imperfect model close to the first bifurcation point $\left(\tilde{u}^*_{4,c}, \mu^*_c\right) = (0.3995, 0.5673)$ for $m = 3$ of the perfect model ; limit point of the imperfect model $\left(\tilde{u}^*_4, \mu^*\right) = (0.397794, 0.565038)$

In the case $4\beta < \alpha$, we have :

$$\sqrt{\frac{1+16\beta}{1+4\alpha}} < 1 < \sqrt{\frac{1+16\beta}{1+4\alpha}}\sqrt{\frac{\alpha}{4\beta}} \tag{58}$$

so that the solution will change in the domain of displacements:

$$\sqrt{\frac{1+16\beta}{1+4\alpha}} \leq \tilde{u}^*_n < 1 \quad \Rightarrow \quad \gamma_2 \geq 1 \quad \Rightarrow \quad -1 \leq 1 - \frac{2}{\gamma_2} < 1 \tag{59}$$

In this case, the solution of Eq. (52) can be written using trigonometric functions:

$$f_{1,2} = \cos\varphi \pm j \sin\varphi \text{ with } \varphi = a\cos\left(1 - \frac{2}{\gamma_2}\right) \tag{60}$$

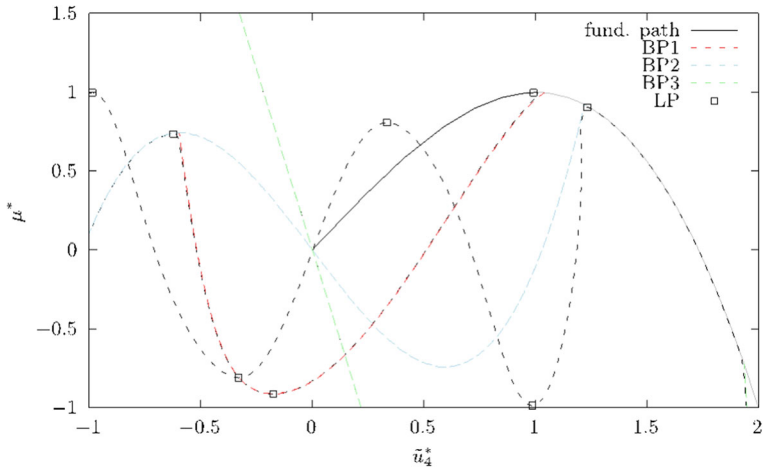

Fig. 17 $n = 4$; $p = 2$; Effect of an imperfection; Imperfection set up on the first non-linear spring of stiffness parameters $(0.99k_1, 0.99M_1)$ between nodes $i = 0$ and $i = 1$; $\alpha = 1/4$; $\beta = 8$; Case $\alpha < 4\beta$; Limit point *LP* of the imperfect model close to the limit point $(\tilde{u}_l^*, \mu_l^*) = (1, 1)$ of the perfect model ; limit point of the imperfect model $(\tilde{u}_4^*, \mu^*) = (0.990709, 0.997422)$

and j is the imaginary number ($j^2 = -1$). The solution of Eq. (47) can then be obtained using trigonometric functions:

$$v_i = A_1 + A_2 i + A_3 \cos(\varphi\, i) + A_{\prime 4} \sin(\varphi\, i) \tag{61}$$

For this range of parameter and considering the four boundary conditions leads to the perturbed solution expressed in trigonometric form:

$$A_1 = A_2 = A_3 = 0 \quad \Rightarrow \quad v_i = A_4 \sin(\varphi\, i) \ \text{ with } \ \sin(\varphi n) = 0 \tag{62}$$

The fundamental solution $A_4 = 0 \quad \Rightarrow \quad v_i = 0$ is still solution of the problem, but some bifurcation values may be obtained from :

$$\varphi = \frac{m\pi}{n} \text{ for } m \in \{1; 2; ...; n-1\} \tag{63}$$

which can be expressed using the dimensionless γ_2 parameter :

$$\gamma_2 = \frac{1}{\sin^2\left(\frac{m\pi}{2n}\right)} \text{ for } m \in \{1; 2; ...; n-1\} \tag{64}$$

We finally obtain an analytical expression for the critical displacement:

$$\left(\tilde{u}_{n,c}^*\right)^2 = \frac{1 - \frac{4\alpha}{1+4\alpha} \sin^2\left(\frac{m\pi}{2n}\right)}{1 - \frac{16\beta}{1+16\beta} \sin^2\left(\frac{m\pi}{2n}\right)} \text{ for } m \in \{1; 2; ...; n-1\} \tag{65}$$

The critical load can be obtained from Eq. (16):

$$\mu_c^* = \frac{\tilde{u}_{n,c}^*}{2}\left[3 - \left(\tilde{u}_{n,c}^*\right)^2\right] \tag{66}$$

In this case, there are *(n-1)* distinct bifurcation parameters before the limit point, which all are contained in the single formulae Eqs. (65) and (66).

It can be checked that for $4\beta < \alpha$:

$$\left(\tilde{u}_{n,c}^*\right)^2 < 1 \text{ for } m \in \{1; 2; ...; n-1\} \tag{67}$$

The bifurcations for this range of parameter $4\beta < \alpha$ prevail before the limit point.

It is easy to check that for the case $n = 2$ and $m = 1$, we obtain the bifurcation parameter already highlighted in the specific study $n = 2$:

$$\left(\tilde{u}^*_{2,c}\right)^2 = \frac{1 - \frac{4\alpha}{1+4\alpha}\sin^2\left(\frac{\pi}{4}\right)}{1 - \frac{16\beta}{1+16\beta}\sin^2\left(\frac{\pi}{4}\right)} = \frac{1 - \frac{2\alpha}{1+4\alpha}}{1 - \frac{8\beta}{1+16\beta}} = \left(\frac{1+2\alpha}{1+4\alpha}\right)\left(\frac{1+16\beta}{1+8\beta}\right) \tag{68}$$

Interestingly, in the general case for various values of n, the smallest bifurcation load for $4\beta < \alpha$ is obtained for the larger mode number:

$$m = n-1 \quad \Rightarrow \quad \left(\tilde{u}^*_{n,c}\right)^2 = \frac{1 - \frac{4\alpha}{1+4\alpha}\cos^2\left(\frac{\pi}{2n}\right)}{1 - \frac{16\beta}{1+16\beta}\cos^2\left(\frac{\pi}{2n}\right)} = \left[\frac{1+16\beta}{1+16\beta\sin^2\left(\frac{\pi}{2n}\right)}\right]\left[\frac{1+4\alpha\sin^2\left(\frac{\pi}{2n}\right)}{1+4\alpha}\right] \tag{69}$$

This smallest bifurcation mode is associated to the buckling mode:

$$m = n-1 \quad \Rightarrow \quad v_i = A_4 \sin\left(\frac{n-1}{n}\pi\, i\right) = A_4\,(-1)^{i+1}\sin\left(\frac{\pi\, i}{n}\right) \tag{70}$$

One recognizes an alternative mode in a trigonometric envelope. For this mode (the one associated to the smallest eigenvalue), the sign changes from one particle to the next. We also point out that this buckling mode valid for the finite FPU chain differs from the so-called microscopic commensurate mode, also based on a sign change from one particle to the next but without the trigonometric envelope, as considered by Truskinovsky and Vainchstein [27] or by Combescure [9] on infinite chain.

For $4\beta = \alpha$, the formulae Eq. (65) is still valid but all bifurcation parameters coalesce in a single value which is the limit point:

$$\alpha = 4\beta \quad \Rightarrow \quad \left(\tilde{u}^*_{n,c}\right)^2 = 1 \text{ for } m \in \{1;\, 2;\, ...;\, n-1\} \tag{71}$$

This is the hill-top bifurcation (degenerate case) studied by Challamel et al. [7] in the particular case $\alpha = \beta = 0$.

In the case $4\beta > \alpha$, we have :

$$\sqrt{\frac{1+16\beta}{1+4\alpha}} > 1 > \sqrt{\frac{1+16\beta}{1+4\alpha}}\sqrt{\frac{\alpha}{4\beta}} \tag{72}$$

so that the solution will change in the domain of displacements:

$$\sqrt{\frac{\alpha}{4\beta}}\sqrt{\frac{1+16\beta}{1+4\alpha}} \le \tilde{u}^*_n < 1 \quad \Rightarrow \quad \gamma_2 \le 0 \quad \Rightarrow \quad 1 - \frac{2}{\gamma_2} > 1 \tag{73}$$

so that the solutions may be equivalently reexpressed by:

$$f_{1,2} = \cosh\theta \pm \sinh\theta \text{ with } \theta = a\cosh\left(1 - \frac{2}{\gamma_2}\right) \tag{74}$$

The solution to Eq. (47) can be finally written as the sum of a linear solution and an exponential:

$$v_i = A_1 + A_2 i + A_3\cosh\left(\theta\, i\right) + A_{\prime 4}\sinh\left(\theta\, i\right) \tag{75}$$

For this range of parameter and considering the four boundary conditions leads to the vanishing perturbed solution (uniqueness of the solution for this range of parameter):

$$A_1 = A_2 = A_3 = A_{\prime 4} = 0 \quad \Rightarrow \quad v_i = 0 \tag{76}$$

It means that in this case, for $4\beta > \alpha$, the bifurcations will act after the limit point $\tilde{u}^*_n = 1$.

To summarize, the FPU system with short and long range interactions possess n critical points obtained from the single formulae:

$$\left(\tilde{u}^*_{n,c}\right)^2 = \frac{1 - \frac{4\alpha}{1+4\alpha}\sin^2\left(\frac{m\pi}{2n}\right)}{1 - \frac{16\beta}{1+16\beta}\sin^2\left(\frac{m\pi}{2n}\right)} \text{ for } m \in \{0;\, 1;\, 2;\, ...;\, n-1\} \tag{77}$$

The case associated to $m = 0$ corresponds to a limit point, whereas the bifurcation points are obtained for $m \in \{1; 2; ...; n-1\}$. For $4\beta > \alpha$, the bifurcations in *(n-1)* (energetically equivalent) unstable bifurcation branches prevail before the limit point. As shown in Appendix A, the initially stable fundamental branch loses its stability at the first critical point, namely for the critical point associated with the highest wave number $m = n-1$. For $4\beta = \alpha$, the bifurcation in *(n-1)* (energetically equivalent) unstable bifurcation branches coincides with the limit point, with an additionnal unstable fundamental branch (n energetically equivalent unstable bifurcation branches). This case is the hill-top bifurcation, already analysed by Challamel et al. [7] in case $p = 1$ (which includes the case $4\beta = \alpha = 0$). When $4\beta < \alpha$, the bifurcations in *(n-1)* (energetically equivalent) unstable bifurcation branches prevail after the limit point, which means that the system becomes first, unstable at the limit point for these values of the structural parameters. As shown in Appendix B, these bifurcation points of the finite generalized FPU system differ from the ones of the infinite system, except for the characterization of the limit point.

These analytical results for the bifurcation values of the generalized FPU lattice with $p = 2$ have been confirmed by a numerical determination of the bifurcation diagram for general n values. The numerical analysis is based on a branch-following software developed by Elliott [13]. The case $n = 4$ is numerically investigated with the two distinct bifurcation diagrams for $\alpha > 4\beta$ and $\alpha < 4\beta$. The analytical bifurcation values presented in Eq. (65) have been obtained in both cases. For $\alpha > 4\beta$ as presented in Fig. 11 and for the specific values of $\alpha = 16$ and $\beta = 0$, the first bifurcation value is obtained for $m = n-1 = 3$ before the limit point *LP* $\left(\tilde{u}_4^*, \mu^*\right) = (1, 1)$, as predicted by the theoretical analysis. The fundamental path loses its stability after this first bifurcation value at $\left(\tilde{u}_{4,c}^*, \mu_c^*, m\right) = (0.3995, 0.5673, 3)$, for the largest value of m. It is numerically observed that this first bifurcated branch (denoted by *BP1*) is unstable. The second bifurcation branch (*BP2*) starts at the critical point $\left(\tilde{u}_{4,c}^*, \mu_c^*, m\right) = (0.7125, 0.8879, 2)$ and the last bifurcation branch (*BP3*) starts at $\left(\tilde{u}_{4,c}^*, \mu_c^*, m\right) = (0.9251, 0.9918, 1)$, which is the closest to the limit point. It is numerically observed, for the parameters of interest, that all bifurcated branches are unstable, according to Lagrange–Dirichlet criterion. For these parameters, a secondary bifurcation has been numerically detected along the branch *BP2* parameterized by $m = 2$, whereas the other branches, parameterized by $m = 1$ and $m = 3$ have no secondary bifurcations (see Fig. 11). In the opposite case, i.e. for $\alpha < 4\beta$ as presented in Fig. 12 for the specific values of $\alpha = 1/4$ and $\beta = 8$, the bifurcation values are reached after the limit point *LP* $\left(\tilde{u}_4^*, \mu^*\right) = (1, 1)$. In this case, the fundamental path loses its stability at the limit point. The first bifurcation value is close to the limit point and is characterized by $m = 1$, for $\left(\tilde{u}_{4,c}^*, \mu_c^*, m\right) = (1.0413, 0.9974, 1)$. Then, the second bifurcation point follows for a larger value of m, i.e. for $\left(\tilde{u}_{4,c}^*, \mu_c^*, m\right) = (1.2200, 0.9221, 2)$ and finally the last bifurcation is characterized by $\left(\tilde{u}_{4,c}^*, \mu_c^*, m\right) = (1.9352, -0.7209, 3)$. For all the cases considered, the closest bifurcation points to the limit point $\left(\tilde{u}_4^*, \mu^*\right) = (1, 1)$ correspond to the smallest value of n (the closest one to $m = 1$). It is also numerically observed in this case, for these parameters of interest, that all bifurcated branches (*BP1*, *BP2* and *BP3*) are unstable, according to Lagrange–Dirichlet criterion. For these parameters, a secondary bifurcation has also been numerically detected along the branch *BP2* parameterized by $m = 2$ (see Fig. 12). It is confirmed, as anticipated by the theoretical analysis, in the case $\alpha > 4\beta$, that the first bifurcation value appears for the larger value of $m = n-1$, which is the bifurcation point the farthest from the limit point. The same analysis is performed for larger values of n, i.e. for instance for $n = 10$ (see Figs. 13, 14 and 15). For $\alpha > 4\beta$ as presented in Fig. 13 and for the specific values of $\alpha = 16$ and $\beta = 0$, the first bifurcation value is obtained for $m = n-1 = 9$ before the limit point *LP* $\left(\tilde{u}_4^*, \mu^*\right) = (1, 1)$, as also predicted by the theoretical analysis. The fundamental path loses its stability after this first bifurcation value at $\left(\tilde{u}_{10,c}^*, \mu_c^*\right) = (0.198695, 0.29412)$, for the largest value of m. It is numerically observed that this first bifurcated branch is unstable. The buckling mode analytically predicted by Eq. (70) associated with a sign function constrained in a sinusoidal envelope is confirmed by the numerical analysis of the fist bifurcation branch in the vicinity of the first bifurcation point, at $\left(\tilde{u}_{10}^*, \mu^*\right) = (0.18805, 0.27662)$ (see Fig. 14). In the opposite case, i.e. for $\alpha < 4\beta$ as presented in Fig. 15 for the specific values of $\alpha = 1/4$ and $\beta = 8$, the bifurcation values are reached after the limit point *LP* $\left(\tilde{u}_4^*, \mu^*\right) = (1, 1)$. In this case, the fundamental path loses its stability at the limit point. The first bifurcation value is close to the limit point *LP* and is characterized by $m = 1$, for $\left(\tilde{u}_{10,c}^*, \mu_c^*\right) = (1.00615, 0.999943)$. The successive bifurcation points are close to each other and forms a cascade of bifurcation points. Figure 15 highlights this characteristic cascade of bifurcation points after the limit point, as already numerically observed

by Triantafyllidis and Bardenhagen [26] for a softening-hardening FPU system with $p = 2$ and with quintic interactions. All the bifurcation branches are not represented in Figs. 13 and 15, which focus more specifically on the bifurcation points which corroborate the previous analytical study.

Furthermore, the generalized FPU system (with direct and indirect interactions) possesses the possible phenomenon of imperfection sensitivity. For $4\beta < \alpha$, and for the parameters of interest, the system has been numerically able to highlight imperfection sensitivity. For the perfect system, the limit load is $\mu^* = 1$, whereas for the imperfect system, even with small imperfection, in the case $4\beta < \alpha$, the limit load would tend towards $\mu^* = \frac{\tilde{u}^*_{n,c}}{2}\left[3 - \left(\tilde{u}^*_{n,c}\right)^2\right] < 1$ with $\tilde{u}^*_{n,c}$ associated with the smallest eigenvalue ($m = n - 1$). Such an imperfection sensitivity phenomenon is illustrated in Fig. 16 for the case $n = 4$, and for $\alpha = 16$ and $\beta = 0$. The imperfection is set up on the first non-linear spring of stiffness parameters $(0.99k_1, 0.99M_1)$ between nodes $i = 0$ and $i = 1$. The equilibrium path does not present a bifurcation point but several limit points LP at which it switches from one perfect bifurcated branch to another. With such a small imperfection, the limit point of the imperfect model $\left(\tilde{u}^*_4, \mu^*\right) = (0.397794, 0.565038)$ is close to the first bifurcation point $\left(\tilde{u}^*_{4,c}, \mu^*_c\right) = (0.3995, 0.5673)$ for $m = n - 1 = 3$ of the perfect model, as expected (see also Fig. 16 where both responses of the perfect and the imperfect models are superposed). On the opposite, for $4\beta > \alpha$, the limit load of the imperfect system is close to unity (the limit load of the perfect model) which may be characteristic of imperfection insensitivity (as numerically shown by Fig. 17 for $n = 4$, and for $\alpha = 1/4$ and $\beta = 8$). Figure 17 also presents both the response of the perfect system and the imperfect one, with a material imperfection introduced in the first non-linear spring. In this sense, the structural boundary $4\beta = \alpha$ is also the boundary between imperfection sensitive to imperfection insensitive systems.

5 About the possibility to capture the bifurcation of the discrete system through a continuum system

The capability to capture these instability phenomena of the discrete FPU system through higher-order continuum theories is discussed in this part. The difference eigenvalue problem can be approximated by a higher-order differential eigenvalue problem thanks to the expansion of the associated pseudo-differential operators up to the fourth-order:

$$v_{i+1} - 2v_i + v_{i-1} = a^2\left[\frac{d^2v}{dx^2} + \frac{a^2}{12}\frac{d^4v}{dx^4}\right] + \mathrm{O}\left(a^6\right) \text{ and } v_{i+2} - 2v_i + v_{i-2} = a^2\left[4\frac{d^2v}{dx^2} + \frac{4a^2}{3}\frac{d^4v}{dx^4}\right] + \mathrm{O}\left(a^6\right) \tag{78}$$

The difference equation Eq. (40) can then be approximated by the following fourth-order gradient elasticity equation:

$$\left[1 - \left(\frac{1+4\alpha}{1+16\beta}\right)\left(\tilde{u}^*_n\right)^2\right]\left[\frac{d^2v}{dx^2} + \frac{a^2}{12}\frac{d^4v}{dx^4}\right] + \left[\alpha - 4\beta\left(\frac{1+4\alpha}{1+16\beta}\right)\left(\tilde{u}^*_n\right)^2\right]\left[4\frac{d^2v}{dx^2} + \frac{4a^2}{3}\frac{d^4v}{dx^4}\right] = 0 \tag{79}$$

which can be rewritten:

$$\left[1 - \left(\tilde{u}^*_n\right)^2\right]\frac{d^2v}{dx^2} + \frac{a^2}{12}\left[\frac{1+16\alpha}{1+4\alpha} - \frac{1+64\beta}{1+16\beta}\left(\tilde{u}^*_n\right)^2\right]\frac{d^4v}{dx^4} = 0 \tag{80}$$

Clearly, the continuum approach is capable of handling the limit point at $\tilde{u}^*_n = 1$. However, the capability of this higher-order continuum approach to predict the bifurcation point depends on the long wave approximation inherent to the asymptotic expansion of the pseudodifferential operators. The continualization of the nonlinear difference equation up to a higher-order is given in Appendix C (nonlinear gradient elasticity model up to order a^4 in the expansion). The boundary conditions expressed in difference form can be also expanded, which gives:

$$v(0) = 0\,;\, \frac{d^2v}{dx^2}(0) = 0;\, v(na) = 0\,;\, \frac{d^2v}{dx^2}(na) = 0 \tag{81}$$

The fourth-order differential equation can be rewritten in the following form, for $\tilde{u}_n^* \neq 1$:

$$\frac{d^4v}{dx^4} + \omega^2 \frac{d^2v}{dx^2} = 0 \text{ with} \frac{1}{\omega^2} = \frac{a^2}{12} \frac{\frac{1+16\alpha}{1+4\alpha} - \frac{1+64\beta}{1+16\beta}\left(\tilde{u}_n^*\right)^2}{1-\left(\tilde{u}_n^*\right)^2} \tag{82}$$

whose solution can be expressed using both the linear function and the trigonometric functions:

$$v(x) = A_1 x + A_2 + A_3 \cos(\omega x) + A_4 \sin(\omega x) \tag{83}$$

Considering the four boundary conditions of the continualized gradient elasticity problem, leads to the perturbed solution expressed in trigonometric form:

$$A_1 = A_2 = A_3 = 0 \quad \Rightarrow \quad v(x) = A_4 \sin(\omega x) \text{ with } \sin(\omega n a) = 0 \tag{84}$$

The gradient elasticity problem has an infinite number of bifurcation values, obtained from :

$$\omega a = \frac{m\pi}{n} \text{ for } m \in \mathrm{N}^* \tag{85}$$

which can be equivalently written as:

$$\frac{(na)^2}{(m\pi)^2} = \frac{a^2}{12} \frac{\frac{1+16\alpha}{1+4\alpha} - \frac{1+64\beta}{1+16\beta}\left(\tilde{u}_n^*\right)^2}{1-\left(\tilde{u}_n^*\right)^2} \tag{86}$$

The gradient elasticity solution (continuum approximation method) for the bifurcation parameters is then expressed by:

$$\left(\tilde{u}_{n,c}^*\right)^2 = \frac{1 - \frac{1}{12}\left(\frac{1+16\alpha}{1+4\alpha}\right)\left(\frac{m\pi}{n}\right)^2}{1 - \frac{1}{12}\left(\frac{1+64\beta}{1+16\beta}\right)\left(\frac{m\pi}{n}\right)^2} \text{ for } m \in \mathrm{N} \tag{87}$$

The gradient elasticity solution (continuous approximation solution) is more accurate for low values of m, as implicitly assumed in the Taylor expansion of the pseudodifferential operator. In fact, the following asymptotic expansion may be performed for the gradient elasticity solution:

$$\frac{m}{n} << 1 \quad \Rightarrow \quad \left(\tilde{u}_{n,c}^*\right)^2 = 1 - \left(\frac{m\pi}{n}\right)^2 \frac{\alpha - 4\beta}{(1+4\alpha)(1+16\beta)} + \mathrm{O}\left(\frac{m}{n}\right)^4 \text{ for } m \in \mathrm{N} \tag{88}$$

For the exact discrete solution, starting from Eq. (65), we obtain the same expansion Eq. (88), which means that the gradient elasticity solution is an asymptotic solution valid for low values of m. In the case $4\beta > \alpha$ where the bifurcation points follow the limit point, this assumption is valid for the first bifurcation points (the first one after the limit point is associated with $m = 1$). However, for $4\beta < \alpha$, the lowest eigenvalue of the discrete problem is obtained for the maximum integer bounded by n (which is out the domain of validity of the expansion assumed in Eq. (88)). As a consequence, the gradient elasticity method loses its efficiency for the bifurcated branches associated with the smallest critical displacements (smallest eigenvalue $\tilde{u}_{n,c}^*$) for $4\beta < \alpha$.

In fact, from Eq. (69) valid for the discrete problem, we have the asymptotic behaviour, for sufficiently large values of n:

$$\begin{aligned} m = n-1 \quad \Rightarrow \quad \lim_{n\to\infty}\left(\tilde{u}_{n,c}^*\right)^2 &= \lim_{n\to\infty} \frac{1 - \frac{4\alpha}{1+4\alpha}\cos^2\left(\frac{\pi}{2n}\right)}{1 - \frac{16\beta}{1+16\beta}\cos^2\left(\frac{\pi}{2n}\right)} \\ = \lim_{n\to\infty}\left[\frac{1+16\beta}{1+16\beta\sin^2\left(\frac{\pi}{2n}\right)}\right]\left[\frac{1+4\alpha\sin^2\left(\frac{\pi}{2n}\right)}{1+4\alpha}\right] &= \frac{1+16\beta}{1+4\alpha} \end{aligned} \tag{89}$$

whereas for the approximated gradient elasticity solution, we have:

$$m = n-1 \quad \Rightarrow \quad \lim_{n\to\infty} \left(\tilde{u}^*_{n,c}\right)^2 = \lim_{n\to\infty} \frac{1 - \frac{1}{12}\left(\frac{1+16\alpha}{1+4\alpha}\right)\left(\frac{m\pi}{n}\right)^2}{1 - \frac{1}{12}\left(\frac{1+64\beta}{1+16\beta}\right)\left(\frac{m\pi}{n}\right)^2}$$

$$= \frac{1 - \frac{\pi^2}{12}\left(\frac{1+16\alpha}{1+4\alpha}\right)}{1 - \frac{\pi^2}{12}\left(\frac{1+64\beta}{1+16\beta}\right)} = \left(\frac{1+16\beta}{1+4\alpha}\right)\left[\frac{1+4\alpha - \frac{\pi^2}{12}(1+16\alpha)}{1+16\beta - \frac{\pi^2}{12}(1+64\beta)}\right] \neq \left(\frac{1+16\beta}{1+4\alpha}\right) \tag{90}$$

The gradient elasticity solution (approximate continuum solution) is able to reproduce the bifurcation behaviour of the discrete FPU chain, especially for the higher bifurcation modes for the considered problem (close to the limit point), but is less accurate for the lower modes associated with the smallest eigenvalues of the discrete problem for $4\beta < \alpha$.

6 Conclusions

In this paper, we studied the bifurcation of a generalized FPU system under pure tension with $p = 2$ nonlinear interactions (nonlinear direct and second-neighbouring interactions). The bifurcation diagram of a generalized FPU system depends on the stiffness ratio of both the linear and the nonlinear parts of the nonlinear lattice, which accounts for both short range and long range interactions. The two dimensionless parameters (dimensionless structural parameters) are $\alpha = k_2/k_1$ the ratio between the stiffnesses of the linear long range interaction and the linear short range interaction, and $\beta = M_2/M_1$, the ratio between the stiffnesses of the nonlinear long range interaction and the nonlinear short range interaction. The bifurcation diagram only depends on these two dimensionless structural parameters. We show that when $4\beta < \alpha$, the bifurcations in *(n-1)* bifurcation branches prevail before the limit point. For $4\beta = \alpha$, the bifurcation in *(n-1)* bifurcation branches coincides with the limit point, with an addition unstable fundamental branch (n energetically equivalent unstable bifurcation branches). This case is the hill-top bifurcation, already analysed by Challamel et al. [7] in case $p = 1$ (which includes the case $4\beta = \alpha = 0$). When $4\beta > \alpha$, the bifurcations in *(n-1)* bifurcation branches prevail after the limit point, which means that the system becomes unstable first, at the limit point. For the parameters of interest, the bifurcation branches have been numerically shown to be instable. The validity of the continuum gradient elasticity approach based on continualization of the difference equations of the initial FPU model is also discussed and appears to be branch-dependent. We also numerically show the possibility for such a generalized FPU system to possess possible imperfection sensitivity. The structural boundary $4\beta = \alpha$ appears to be the boundary between imperfection sensitive to imperfection insensitive systems.

Author contribution Noël Challamel, Christelle Combescure, Vincent Picandet, Manuel Ferretti and Angelo Luongo contributed to the elaboration of results, including analytical results, numerical results and graphical representation.

Data availibility No datasets were generated or analysed during the current study.

Funding Open access funding provided by Université de Bretagne Sud.

Declarations

Conflict of interest The authors declare no competing interests.

Appendix A: Stability of the discrete FPU system

In this appendix, the instability of the fundamental path after the bifurcation will be shown, from the application of Lagrange–Dirichlet theorem of instability (from the loss of the definite positiveness of the discrete potential energy). We start from the potential energy Eq. (1) which is rewritten here in the following form:

$$\begin{aligned} W = & \sum_{i=1}^{n-1} \frac{k_1}{4} \left[(u_{i+1} - u_i)^2 + (u_i - u_{i-1})^2 \right] - \frac{M_1}{8a^2} \left[(u_{i+1} - u_i)^4 + (u_i - u_{i-1})^4 \right] \\ & + \frac{k_1}{4} (u_1 - u_0)^2 - \frac{M_1}{8a^2} (u_1 - u_0)^4 + \frac{k_1}{4} (u_n - u_{n-1})^2 - \frac{M_1}{8a^2} (u_n - u_{n-1})^4 \\ & + \sum_{i=1}^{n-1} \frac{k_2}{4} \left[(u_{i+2} - u_i)^2 + (u_i - u_{i-2})^2 \right] - \frac{M_2}{8a^2} \left[(u_{i+2} - u_i)^4 + (u_i - u_{i-2})^4 \right] \\ & + \lambda_1 u_0 + \lambda_2 (u_n - \overline{u_n}) + \lambda_3 (u_1 + u_{-1}) + \lambda_4 (u_{n+1} - 2u_n + u_{n-1}) \end{aligned} \tag{A1}$$

If the boundary terms are omitted in the proof for simplification of the writing, the energy potential is rewritten:

$$\begin{aligned} W = & \sum_{i} \frac{k_1}{4} \left[(u_{i+1} - u_i)^2 + (u_i - u_{i-1})^2 \right] - \frac{M_1}{8a^2} \left[(u_{i+1} - u_i)^4 + (u_i - u_{i-1})^4 \right] \\ & + \sum_{i} \frac{k_2}{4} \left[(u_{i+2} - u_i)^2 + (u_i - u_{i-2})^2 \right] - \frac{M_2}{8a^2} \left[(u_{i+2} - u_i)^4 + (u_i - u_{i-2})^4 \right] \end{aligned} \tag{A2}$$

We use the following change of variable, already considered in Eq. (37):

$$v_i = u_i - \overline{u} \frac{i}{n} \tag{A3}$$

The potential energy is expressed in its nonlinear form with the new perturbed displacement variable around the homogeneous solution:

$$\begin{aligned} W = & \sum_{i} \frac{k_1}{4} \left[(v_{i+1} - v_i)^2 + (v_i - v_{i-1})^2 + 2\frac{\overline{u}}{n} (v_{i+1} - v_{i-1}) + 2 \left(\frac{\overline{u}}{n} \right)^2 \right] \\ & - \sum_{i} \frac{M_1}{8a^2} \left[\begin{array}{l} (v_{i+1} - v_i)^4 + (v_i - v_{i-1})^4 + 4\frac{\overline{u}}{n} \left[(v_{i+1} - v_i)^3 + (v_i - v_{i-1})^3 \right] + \\ 6 \left(\frac{\overline{u}}{n} \right)^2 \left[(v_{i+1} - v_i)^2 + (v_i - v_{i-1})^2 \right] + 4 \left(\frac{\overline{u}}{n} \right)^3 (v_{i+1} - v_{i-1}) + 2 \left(\frac{\overline{u}}{n} \right)^4 \end{array} \right] \\ & + \sum_{i} \frac{k_2}{4} \left[(v_{i+2} - v_i)^2 + (v_i - v_{i-2})^2 + 4\frac{\overline{u}}{n} (v_{i+2} - v_{i-2}) + 8 \left(\frac{\overline{u}}{n} \right)^2 \right] \\ & - \sum_{i} \frac{M_2}{8a^2} \left[\begin{array}{l} (v_{i+2} - v_i)^4 + (v_i - v_{i-2})^4 + 8\frac{\overline{u}}{n} \left[(v_{i+2} - v_i)^3 + (v_i - v_{i-2})^3 \right] \\ +24 \left(\frac{\overline{u}}{n} \right)^2 \left[(v_{i+2} - v_i)^2 + (v_i - v_{i-2})^2 \right] + 32 \left(\frac{\overline{u}}{n} \right)^3 (v_{i+2} - v_{i-2}) + 32 \left(\frac{\overline{u}}{n} \right)^4 \end{array} \right] \end{aligned} \tag{A4}$$

We only consider the quadratic approximation associated to the linearized difference form for the governing difference equations (the constant terms and the first-order terms do not affect the governing difference equations):

$$\begin{aligned} W = & \sum_{i} \frac{1}{4} \left[k_1 - 3M_1 \left(\frac{\overline{u}}{na} \right)^2 \right] \left[(v_{i+1} - v_i)^2 + (v_i - v_{i-1})^2 \right] \\ & + \sum_{i} \frac{1}{4} \left[k_2 - 12M_2 \left(\frac{\overline{u}}{na} \right)^2 \right] \left[(v_{i+2} - v_i)^2 + (v_i - v_{i-2})^2 \right] \end{aligned} \tag{A5}$$

The quadratic approximation of the potential energy Eq. (A5) can be also rewritten in a more synthetic form:

$$W = \sum_i \frac{1}{2}\left[k_1 - 3M_1\left(\frac{\overline{u}}{na}\right)^2\right](v_{i+1} - v_i)^2 + \sum_i \frac{1}{2}\left[k_2 - 12M_2\left(\frac{\overline{u}}{na}\right)^2\right](v_{i+2} - v_i)^2 \tag{A6}$$

This potential energy can be also rewritten using some symmetrical difference operators:

$$\begin{aligned} W = &\sum_{i=1/2}^{n-1/2} \frac{1}{2}\left[k_1 - 3M_1\left(\frac{\overline{u}}{na}\right)^2\right]\left(v_{i+1/2} - v_{i-1/2}\right)^2 + \sum_{i=0}^{n} \frac{1}{2}\left[k_2 - 12M_2\left(\frac{\overline{u}}{na}\right)^2\right](v_{i+1} - v_{i-1})^2 \\ &-\frac{1}{4}\left[k_2 - 12M_2\left(\frac{\overline{u}}{na}\right)^2\right](v_1 - v_{-1})^2 - \frac{1}{4}\left[k_2 - 12M_2\left(\frac{\overline{u}}{na}\right)^2\right](v_{n+1} - v_{n-1})^2 \end{aligned} \tag{A7}$$

This potential energy can be equivalently rewritten using left and right difference operators for the direct neighboring interaction:

$$\begin{aligned} W = &\sum_{i=0}^{n} \frac{1}{4}\left[k_1 - 3M_1\left(\frac{\overline{u}}{na}\right)^2\right]\left[(v_{i+1} - v_i)^2 + (v_i - v_{i-1})^2\right] + \sum_{i=0}^{n} \frac{1}{2}\left[k_2 - 12M_2\left(\frac{\overline{u}}{na}\right)^2\right](v_{i+1} - v_{i-1})^2 \\ &-\frac{1}{4}\left[k_1 - 3M_1\left(\frac{\overline{u}}{na}\right)^2\right]\left[(v_0 - v_{-1})^2 + (v_{n+1} - v_n)^2\right] - \frac{1}{4}\left[k_2 - 12M_2\left(\frac{\overline{u}}{na}\right)^2\right] \\ &\left[(v_1 - v_{-1})^2 + (v_{n+1} - v_{n-1})^2\right] \end{aligned} \tag{A8}$$

It is also possible to express the second term of this quadratic potential energy using both the first-order difference and the second-order difference operator:

$$\begin{aligned} W = &\sum_{i=0}^{n} \frac{1}{4}\left[k_1 - 3M_1\left(\frac{\overline{u}}{na}\right)^2\right]\left[(v_{i+1} - v_i)^2 + (v_i - v_{i-1})^2\right] \\ &+\sum_{i=0}^{n} \frac{1}{2}\left[k_2 - 12M_2\left(\frac{\overline{u}}{na}\right)^2\right]\left[2\,(v_{i+1} - v_i)^2 + 2\,(v_i - v_{i-1})^2 - (v_{i+1} - 2v_i + v_{i-1})^2\right] \\ &-\frac{1}{4}\left[k_1 - 3M_1\left(\frac{\overline{u}}{na}\right)^2\right]\left[(v_0 - v_{-1})^2 + (v_{n+1} - v_n)^2\right] - \frac{1}{4}\left[k_2 - 12M_2\left(\frac{\overline{u}}{na}\right)^2\right] \\ &\left[(v_1 - v_{-1})^2 + (v_{n+1} - v_{n-1})^2\right] \end{aligned} \tag{A9}$$

Using the macroscopic stiffness parameters $k = k_1 + 4k_2$ and $M = M_1 + 16M_2$, and including the higher-order boundary conditions expressed in difference form (antisymmetrical higher-order boundary conditions), we finally obtain the equivalent quadratic approximation of the potential energy :

$$W = \sum_{i=0}^{n-1} \frac{1}{2}\left[k - 3M\left(\frac{\overline{u}}{na}\right)^2\right](v_{i+1} - v_i)^2 - \sum_{i=1}^{n-1} \frac{1}{2}\left[k_2 - 12M_2\left(\frac{\overline{u}}{na}\right)^2\right](v_{i+1} - 2v_i + v_{i-1})^2 \tag{A10}$$

which can be also expressed equivalently using symmetrical difference operators:

$$W = \sum_{i=1/2}^{n-1/2} \frac{1}{2}\left[k - 3M\left(\frac{\overline{u}}{na}\right)^2\right]\left(v_{i+1/2} - v_{i-1/2}\right)^2 - \sum_{i=1}^{n-1} \frac{1}{2}\left[k_2 - 12M_2\left(\frac{\overline{u}}{na}\right)^2\right](v_{i+1} - 2v_i + v_{i-1})^2 \tag{A11}$$

The stationatity of the quadratic approximation of the potential energy $\delta W = 0$ gives the linearized fourth-order difference equation:

$$\left[k - 3M\left(\frac{\overline{u}}{na}\right)^2\right]\left(v_{i+1} - 2v_i + v_{i-1}\right) + \left[k_2 - 12M_2\left(\frac{\overline{u}}{na}\right)^2\right]\left(v_{i+2} - 4v_{i+1} + 6v_i - 4v_{i-1} + 6v_{i-2}\right) = 0 \tag{A12}$$

which has been obtained equivalently in Eq. (39) from the direct linearization of the fourth-order nonlinear governing difference equations.
We are interested by the property of the second variation of the associated potential energy, in order to characterize the stability of the fundamental path before and after the bifurcation parameters. The second variation of the potential energy is calculated as:

$$\delta^2 W = \sum_{i=1/2}^{n-1/2}\left[k - 3M\left(\frac{\overline{u}}{na}\right)^2\right]\left(\delta v_{i+1/2} - \delta v_{i-1/2}\right)^2 - \sum_{i=1}^{n-1}\left[k_2 - 12M_2\left(\frac{\overline{u}}{na}\right)^2\right]\left(\delta v_{i+1} - 2\delta v_i + \delta v_{i-1}\right)^2 \tag{A13}$$

We first consider the case $4\beta < \alpha$, where bifurcation prevails at $\tilde{u}_n^* = \tilde{u}_{n,c}^*$ before the limit point $\tilde{u}_n^* = 1$. We will show that the potential energy is no more definite positive for some critical values $\tilde{u}_n^* = \tilde{u}_{n,c}^*$, which means, according to Lagrange–Dirichlet criterion, that the fundamental path is unstable above this bifurcation parameter (see for instance [2,21,23]).

$$\tilde{u}_n^* > \tilde{u}_{n,c}^* \quad \Rightarrow \quad \exists\,(\delta v_i) \;/\; \delta^2 W < 0 \tag{A14}$$

Pflüger [23] for instance used a similar reasoning to show the instability of the *elastica* above the Euler buckling load. For the proof, we consider the discrete displacement field:

$$\delta v_i = \delta V_m \sin\frac{m\pi\, i}{n} \text{ with } m = n - 1 \tag{A15}$$

which verifies the boundary conditions

$$\delta v_0 = 0; \quad \delta v_n = 0 \quad ; \quad \delta v_{-1} = -\delta v_1 \text{ and } \delta v_{n-1} = -\delta v_{n+1} \tag{A16}$$

For such a kinematic field, the second variation of the potential energy is calculated as:

$$\begin{aligned}\delta^2 W = &\left[k - 3M\left(\frac{\overline{u}}{na}\right)^2\right](\delta V_m)^2\, 4\sin^2\frac{m\pi}{2n}\sum_{i=1/2}^{n-1/2}\cos^2\frac{m\pi\, i}{n} \\ &- \left[k_2 - 12M_2\left(\frac{\overline{u}}{na}\right)^2\right](\delta V_m)^2\, 16\sin^4\frac{m\pi}{2n}\sum_{i=1}^{n-1}\sin^2\frac{m\pi\, i}{n}\end{aligned} \tag{A17}$$

We use the fundamental property:

$$\sum_{i=1}^{n-1}\sin^2\left(\frac{m\pi\, i}{n}\right) = \frac{n}{2} \text{ and } \sum_{i=1/2}^{n-1/2}\cos^2\frac{m\pi\, i}{n} = \frac{n}{2} \tag{A18}$$

For such a kinematic field, the second variation of energy is calculated as:

$$\delta^2 W = 2nk\sin^2\frac{m\pi}{2n}(\delta V_m)^2\left[1 - 3\frac{M}{k}\left(\frac{\overline{u}}{na}\right)^2 - 4\sin^2\frac{m\pi}{2n}\left[\frac{k_2}{k} - 12\frac{M_2}{k}\left(\frac{\overline{u}}{na}\right)^2\right]\right] \tag{A19}$$

If we consider the critical buckling mode:

$$m = n - 1 \quad \Rightarrow \quad \delta^2 W = 2nk\cos^2\frac{\pi}{2n}(\delta V_m)^2\left[1 - 3\frac{M}{k}\left(\frac{\overline{u}}{na}\right)^2 - 4\cos^2\frac{\pi}{2n}\left[\frac{k_2}{k} - 12\frac{M_2}{k}\left(\frac{\overline{u}}{na}\right)^2\right]\right] \tag{A20}$$

We finally obtain the instability result for $4\beta < \alpha$:

$$\left(\tilde{u}_n^*\right)^2 > \left(\tilde{u}_{n,c}^*\right)^2 = \frac{1 - 4\frac{k_2}{k}\cos^2\frac{\pi}{2n}}{1 - 16\frac{M_2}{M}\cos^2\frac{\pi}{2n}} \quad \Rightarrow \quad \delta^2 W < 0 \tag{A21}$$

For $\tilde{u}_n^* > \tilde{u}_{n,c}^*$, the fundamental path is unstable, according to the instability theorem of Lagrange–Dirichlet (loss of stability of the fundamental path after the bifurcation point $\tilde{u}_n^* = \tilde{u}_{n,c}^*$). We note that for $4\beta < \alpha$, $\tilde{u}_n^* = \tilde{u}_{n,c}^*$ is smaller than unity, which means that the bifurcation prevails before the limit point.
On the other hand, for $4\beta > \alpha$, the instability prevails at the limit point which precedes the bifurcation point:

$$\tilde{u}_n^* > 1 \Rightarrow \quad \delta^2 W < 0 \tag{A22}$$

In fact, it is possible to show from an asymptotic expansion, that:

$$m \to 0 \quad \Rightarrow \quad \delta^2 W = 2nk\left(\frac{m\pi}{2n}\right)^2 (\delta V_m)^2 \left[1 - 3\frac{M}{k}\left(\frac{\overline{u}}{na}\right)^2\right] \tag{A23}$$

In this case, the sign of the second variation of the total potential energy is controlled by the value of the displacement at the limit point.
To complete the proof, and to show the stability of the fundamental path below the bifurcation value, for $4\beta < \alpha$, one should show that:

$$\left(\tilde{u}_n^*\right)^2 < \left(\tilde{u}_{n,c}^*\right)^2 = \frac{1 - \frac{4\alpha}{1+4\alpha}\cos^2\frac{\pi}{2n}}{1 - \frac{16\beta}{1+16\beta}\cos^2\frac{\pi}{2n}} \quad \Rightarrow \quad \delta^2 W > 0 \ \ \forall\, (\delta v_i) \tag{A24}$$

We will follow the reasoning presented by Bažant and Cedolin [2] for the stability proof of the continuous elastica, according to Lagrange-Dirichlet criterion. The kinematic field is expanded using the complete trigonometric base:

$$\delta v_i = \sum_{m=1}^{n-1} \delta V_m \sin\frac{m\pi\, i}{n} \tag{A25}$$

We inject this kinematic field in the second variation of energy:

$$\begin{aligned}\delta^2 W = &\sum_{i=1/2}^{n-1/2}\left[k - 3M\left(\frac{\overline{u}}{na}\right)^2\right]\left(\sum_{m=1}^{n-1} 2\sin\frac{m\pi}{2n}\delta V_m \cos\frac{m\pi\, i}{n}\right)^2 \\ &- \sum_{i=1}^{n-1}\left[k_2 - 12M_2\left(\frac{\overline{u}}{na}\right)^2\right]\left(\sum_{m=1}^{n-1}\left[2\cos\frac{m\pi}{n} - 2\right]\delta V_m \sin\frac{m\pi\, i}{n}\right)^2\end{aligned} \tag{A26}$$

The square of the sum is simplified into the sum of each square term, due to the orthogonality of each mode (as also detailed by Bažant and Cedolin, [2] for the continuous elastica problem – the same properties also hold in the discrete problem investigated in this paper), which is expressed by the orthogonality condition:

$$\sum_{i\,=\,1/2\ m\,\neq\,p}^{n-1/2} \cos\left(\frac{m\pi\, i}{n}\right)\cos\left(\frac{p\pi\, i}{n}\right) = 0 \text{ and } \sum_{\substack{i\,=\,1 \\ m\,\neq\,p}}^{n-1} \sin\left(\frac{m\pi\, i}{n}\right)\sin\left(\frac{p\pi\, i}{n}\right) = 0 \tag{A27}$$

The second variation of energy is then rewritten:

$$\begin{aligned}\delta^2 W = &\left[k - 3M\left(\frac{\overline{u}}{na}\right)^2\right]\sum_{i=1/2}^{n-1/2}\sum_{m=1}^{n-1} 4\sin^2\frac{m\pi}{2n}(\delta V_m)^2\cos^2\frac{m\pi\, i}{n} \\ &- \left[k_2 - 12M_2\left(\frac{\overline{u}}{na}\right)^2\right]\sum_{i=1}^{n-1}\sum_{m=1}^{n-1} 16\sin^4\frac{m\pi}{2n}(\delta V_m)^2\sin^2\frac{m\pi\, i}{n}\end{aligned} \tag{A28}$$

Using again the fundamental properties of the sum of trigonometric functions presented in Eq. (A18), we obtain:

$$\delta^2 W = \sum_{m=1}^{n-1} 2n \sin^2 \frac{m\pi}{2n} (\delta V_m)^2 \left[k - 3M \left(\frac{\overline{u}}{na} \right)^2 - 4 \sin^2 \frac{m\pi}{2n} \left[k_2 - 12 M_2 \left(\frac{\overline{u}}{na} \right)^2 \right] \right] \tag{A29}$$

which is a generalization of Eq. A19 valid for one mode. The second variation of energy can be rewritten:

$$\delta^2 W = k \sum_{m=1}^{n-1} 2n \sin^2 \frac{m\pi}{2n} (\delta V_m)^2 \left(1 - \frac{16\beta}{1+16\beta} \sin^2 \frac{m\pi}{2n} \right) \left[\frac{1 - \frac{4\alpha}{1+\alpha} \sin^2 \frac{m\pi}{2n}}{1 - \frac{16\beta}{1+16\beta} \sin^2 \frac{m\pi}{2n}} - \left(\tilde{u}_n^* \right)^2 \right] \tag{A30}$$

It is obvious to check that:

$$\left(\tilde{u}_n^* \right)^2 \leq \min_{m \in \{1,..,n-1\}} \frac{1 - \frac{4\alpha}{1+\alpha} \sin^2 \frac{m\pi}{2n}}{1 - \frac{16\beta}{1+16\beta} \sin^2 \frac{m\pi}{2n}} = \frac{1 - \frac{4\alpha}{1+\alpha} \cos^2 \frac{\pi}{2n}}{1 - \frac{16\beta}{1+16\beta} \cos^2 \frac{\pi}{2n}} = \left(\tilde{u}_{n,c}^* \right)^2 \quad \Rightarrow \quad \delta^2 W > 0 \; \forall \left(\delta v_i \right) \tag{A31}$$

As a consequence, the second variation of the potential energy is definite positive before the bifurcation point which means that the fundamental path is stable before the bifurcation point for $4\beta < \alpha$ (where the bifurcation point prevails before the limit point), according to the stability theorem of Lagrange-Dirichlet. On the other hand, for $4\beta > \alpha$, the limit point prevails before the bifurcation point, which is illustrated by the definite positivity property :

$$\left(\tilde{u}_n^* \right)^2 \leq \min_{m \in \{0,1,..,n-1\}} \frac{1 - \frac{4\alpha}{1+\alpha} \sin^2 \frac{m\pi}{2n}}{1 - \frac{16\beta}{1+16\beta} \sin^2 \frac{m\pi}{2n}} = 1 \quad \Rightarrow \quad \delta^2 W > 0 \; \forall \left(\delta v_i \right) \tag{A32}$$

Appendix B: Comparison between the finite and the infinite generalized FPU system

The potential energy associated with each interaction ($p = 1$ and $p = 2$ interactions) can be presented from the quartic function:

$$w_p(\varepsilon) = \frac{1}{2} \tilde{K}_p \varepsilon^2 - \frac{\tilde{M}_p}{4} \varepsilon^4 \text{ with } \tilde{K}_p = p K_p \text{ and } \tilde{M}_p = p^3 M_p \tag{B1}$$

where ε is a strain variable (difference of displacements in the chain normalized by the length of the element). The stiffness function $g_p(\varepsilon)$ can be introduced following the notation of Truskinovsky and Vainchstein [27]:

$$g_p(\varepsilon) = \frac{w_p''(\varepsilon)}{p} = \frac{\tilde{K}_p}{p} - \frac{3\tilde{M}_p}{p} \varepsilon^2 \tag{B2}$$

Truskinovsky and Vainchstein [27] or Combescure [9] derived the long wavelength instability criterion of the infinite chain (critical strain along the fundamental homogeneous path), which coincides with the limit point for the present finite chain:

$$\sum_{p=1}^{2} p^2 g_p \left(\varepsilon^0 \right) = g_1 \left(\varepsilon^0 \right) + 4 g_2 \left(\varepsilon^0 \right) = 0 \tag{B3}$$

which is equivalently written:

$$\left(\varepsilon^0 \right)^2 = \frac{K_1 + 4K_2}{3 \left(M_1 + 16 M_2 \right)} = \frac{K}{3M} = \tilde{u}_l^2 \tag{B4}$$

Noting that the critical strain can be reexpressed in term of dimensionless displacement $\varepsilon^0 = \tilde{u}_n$, the long wavelength instability criterion coincides with the limit point (which is also valid for the finite problem):

$$\tilde{u}_n^* = 1 \tag{B5}$$

The short wavelength instability (called microscopic commensurate by Truskinovsky and Vainchstein, [27]) of the infinite chain can be obtained from (see again Truskinovsky and Vainchstein, [27] or Combescure, [9]):

$$g_1\left(\varepsilon^0\right) = 0 \tag{B6}$$

This last instability criterion can be written for the quintic interaction considered in the paper as:

$$\left(\varepsilon^0\right)^2 = \frac{K_1}{3M_1} \tag{B7}$$

which is associated with the critical dimensionless displacement:

$$\left(\tilde{u}_n^*\right)^2 = \frac{1+16\beta}{1+4\alpha} \tag{B8}$$

This critical value valid for the infinite system differs from the exact bifurcation values given by Eq. (65) for the finite system, except for $m = n$, which is not a bifurcation value of the finite system. However, even if the finite and the infinite system differ, we note that for $4\beta < \alpha$, the first bifurcation value is obtained for $m = n - 1$, which means that, according to Eq. (89) :

$$\begin{aligned} m = n-1 \quad \Rightarrow \quad \lim_{n\to\infty}\left(\tilde{u}_{n,c}^*\right)^2 &= \lim_{n\to\infty}\frac{1-\frac{4\alpha}{1+4\alpha}\cos^2\left(\frac{\pi}{2n}\right)}{1-\frac{16\beta}{1+16\beta}\cos^2\left(\frac{\pi}{2n}\right)} \\ = \lim_{n\to\infty}\left[\frac{1+16\beta}{1+16\beta\sin^2\left(\frac{\pi}{2n}\right)}\right]\left[\frac{1+4\alpha\sin^2\left(\frac{\pi}{2n}\right)}{1+4\alpha}\right] &= \frac{1+16\beta}{1+4\alpha} \end{aligned} \tag{B9}$$

Eq. (B9) confirms how the first bifurcation value of the discrete system converges towards the theoretical value of the infinite system.
It is also quite interesting to comment to instability mode of the infinite system, as compared to the one of the finite system. The linearized fourth-order difference equation is given by Eq. (47):

$$v_{i+1} - 2v_i + v_{i-1} + \frac{\gamma_2}{4}\left(v_{i+2} - 4v_{i+1} + 6v_i - 4v_{i-1} + v_{i-2}\right) = 0 \text{ with } \gamma_2 = \frac{\frac{4\alpha}{1+4\alpha} - \frac{16\beta\left(\tilde{u}_n^*\right)^2}{1+16\beta}}{1-\left(\tilde{u}_n^*\right)^2} \tag{B10}$$

The short wavelength instability mode is given, for the infinite chain, by (see Truskinovsky and Vainchstein, [27]):

$$v_i = A_4\,(-1)^i \tag{B11}$$

We note that this mode does not fulfill the boundary conditions of the problem and cannot be used for the finite problem. Injecting Eq. (B11) in Eq. (B10) gives the elementary solution:

$$\gamma_2 = 1 \quad \Rightarrow \quad \left(\tilde{u}_n^*\right)^2 = \frac{1+16\beta}{1+4\alpha} \tag{B12}$$

As a conclusion, it is shown here how the finite FPU system differs from the infinite one, in term of bifurcation values, and how the infinite system may be used as an asymptotic case of the finite system.

Appendix C: Continualization of the nonlinear difference equation up to higher-order terms

The nonlinear difference equation Eq. (38) can be continualized using the asymptotic expansion of the associated pseudodifferential operators:

$$\begin{aligned}
&k_1 \left(v_{i+1} - 2v_i + v_{i-1}\right) \\
&\quad -\frac{M_1}{a^2}\left(v_{i+1} - 2v_i + v_{i-1}\right)\left[\left(v_{i+1} - v_i\right)^2 + \left(v_{i+1} - v_i\right)\left(v_i - v_{i-1}\right) + \left(v_i - v_{i-1}\right)^2\right. \\
&\quad \left. +3\frac{\overline{u}}{n}\left(v_{i+1} - v_{i-1}\right) + 3\left(\frac{\overline{u}}{n}\right)^2\right] \\
&\quad +k_2 \left(v_{i+2} - 2v_i + v_{i-2}\right) \\
&\quad -\frac{M_2}{a^2}\left(v_{i+2} - 2v_i + v_{i-2}\right)\left[\left(v_{i+2} - v_i\right)^2 + \left(v_{i+2} - v_i\right)\left(v_i - v_{i-2}\right) + \left(v_i - v_{i-2}\right)^2\right. \\
&\quad \left. +6\frac{\overline{u}}{n}\left(v_{i+2} - v_{i-2}\right) + 12\left(\frac{\overline{u}}{n}\right)^2\right] \\
&\quad = 0
\end{aligned} \tag{C1}$$

An expansion of Eq. (C1) up to order a^4 gives the nonlinear gradient elasticity equation:

$$\begin{aligned}
&k_1\left[v'' + \frac{a^2}{12}v^{(4)}\right] + k_2\left[4v'' + \frac{4a^2}{3}v^{(4)}\right] \\
&-M_1\left[\begin{array}{l} 3\left(v'\right)^2 v'' + a^2 v' v'' v''' + \frac{a^2}{4}\left(v''\right)^3 + \frac{3\overline{u}}{na}\left(2v'v'' + \frac{a^2}{3}v''v'''\right) \\ \quad +3\left(\frac{\overline{u}}{na}\right)^2 v'' + \frac{a^2}{4}v^{(4)}\left(v'\right)^2 + \frac{6\overline{u}}{na}v'\frac{a^2}{12}v^{(4)} + 3\left(\frac{\overline{u}}{na}\right)^2\frac{a^2}{12}v^{(4)} \end{array}\right] \\
&-M_2\left[\begin{array}{l} 48\left(v'\right)^2 v'' + 64a^2 v' v'' v''' + 16a^2\left(v''\right)^3 + \frac{6\overline{u}}{na}\left(16v'v'' + \frac{32a^2}{3}v''v'''\right) \\ +48\left(\frac{\overline{u}}{na}\right)^2 v'' + \frac{48a^2}{3}v^{(4)}\left(v'\right)^2 + \frac{6\overline{u}}{na}v'\frac{16a^2}{3}v^{(4)} + 48\left(\frac{\overline{u}}{na}\right)^2\frac{a^2}{3}v^{(4)} \end{array}\right] = 0
\end{aligned} \tag{C2}$$

Higher-order differential equations may be theoretically derived from expansion of the difference operators up to higher orders. This nonlinear fourth-order differential equation can be linearized to give:

$$\begin{aligned}
&\left(k_1 + 4k_2\right)v'' + \frac{a^2}{12}\left(k_1 + 16k_2\right)v^{(4)} \\
&\quad -\left(\frac{\overline{u}}{na}\right)^2\left(3M_1 + 48M_2\right)v'' - \left(\frac{\overline{u}}{na}\right)^2\frac{a^2}{12}\left(3M_1 + 192M_2\right)v^{(4)} = 0
\end{aligned} \tag{C3}$$

This fourth-order linearized differential equation can be normalized as:

$$\begin{aligned}
&v'' + \frac{a^2}{12}\frac{k_1 + 16k_2}{k_1 + 4k_2}v^{(4)} \\
&\quad -3\left(\frac{\overline{u}}{na}\right)^2\frac{M_1 + 16M_2}{k_1 + 4k_2}v'' - 3\left(\frac{\overline{u}}{na}\right)^2\frac{a^2}{12}\frac{M_1 + 64M_2}{k_1 + 4k_2}v^{(4)} = 0
\end{aligned} \tag{C4}$$

which coincides with Eq. (80):

$$\begin{aligned}
&\left[1 - \left(\tilde{u}_n^*\right)^2\right]\frac{d^2v}{dx^2} + \frac{a^2}{12}\left[\frac{1 + 16\alpha}{1 + 4\alpha} - \frac{1 + 64\beta}{1 + 16\beta}\left(\tilde{u}_n^*\right)^2\right]\frac{d^4v}{dx^4} = 0 \text{ with } \left(\tilde{u}_n^*\right)^2 = 3\frac{M}{k}\left(\frac{\overline{u}}{na}\right)^2, \\
&\alpha = \frac{k_2}{k_1} \text{ and } \beta = \frac{M_2}{M_1}
\end{aligned} \tag{C5}$$

References

1. Andrianov, I.V., Awrejcewicz, J., Danishevskyy, V.: Linear and nonlinear waves in microstructured solids—Homogenization and asymptotic approaches. CRC Press, Boca Raton (2021)
2. Bažant, Z.P., Cedolin, L.: Stability of structures–elastic, inelastic, fracture and damage theories. Dover Publications, Inc., New York (2003)
3. Challamel, N., Wang, C.M., Elishakoff, I.: Discrete systems behave as nonlocal structural elements: bending, buckling and vibration analysis. Eur. J. Mech. A/Solids **44**, 125–135 (2014)
4. Challamel, N., Wang, C.M., Zhang, H., Kitipornchai, S.: Exact and nonlocal solutions for vibration of axial lattices with direct and indirect neighbouring interactions. J. Eng., Mech. **144**(5), 04018025 (2018)
5. Challamel, N., Zhang, H., Wang, C.M., Kaplunov, J.: Scale effect and higher-order boundary conditions for generalized lattices, with direct and indirect interactions. Mech. Res. Commun. **97**, 1–7 (2019)
6. Challamel, N., and Picandet, V.: Localization in the static response of higher-order lattices with long range interactions. In: Challamel, N., Kaplunov, J., and Takewaki, I. (Eds), *Modern Trends in Structural and Solid Mechanics 1*. – Statics and Stability, pp. 67-89, ISTE-Wiley, (2021)
7. Challamel, N., Ferretti, M., Luongo, A.: Multi-degenerate hill-top bifurcation of Fermi–Pasta–Ulam softening chains: exact and asymptotic solutions. Int. J. Non-Linear Mech. **156**(104509), 1–11 (2023)
8. Charlotte, M., Truskinovsky, L.: Linear elastic chain with a hyper-pre-stress. J. Mech. Phys. Solids **50**, 217–251 (2002)
9. Combescure, C.: Selecting generalized continuum theories for nonlinear periodic solids based on the instabilities of the underlying microstructure. J Elast **154**, 421–441 (2023)
10. Eaton, H.C., Peddieson, J., Jr.: On continuum description of one-dimensional lattice mechanics. J. Tennessee Acad. Sci. **48**(3), 96–100 (1973)
11. Friedman, N., Weiner, M., Farkas, G., Hegedüs, I., Ibrahimbegovic, A.: On the snap-back behavior of a self-deploying antiprismatic column during packing. Eng. Struct. **50**, 74–89 (2013)
12. Elaydi, S.: *An introduction to difference equations*, 3rd edn., Springer, (2005)
13. Elliott, R.S.: Multiscale bifurcation and stability of multilattices. J. Comput.-Aided Mater. Des. **14**(1), 143–157 (2007)
14. Fermi, E., Pasta, J., Ulam, S.: Studies of nonlinear problems. Los Alamos Rep. **1940**, 978 (1955)
15. Gazis, D.C., Wallis, R.F.: Surface tension and surface modes in semi-infinite lattices. Surf. Sci. **3**, 19–32 (1964)
16. Goldberg, S.: Introduction to difference equations with illustrative examples from economics, psychology and sociology. Dover Publications, New-York (1958)
17. Hencky, H.: Über die angenäherte Lösung von Stabilitätsproblemen im Raummittels der elastischen Gelenkkette. Der Eisenbau **11**, 437–452 (1920)
18. Kruskal, M.D., Zabusky, N.J.: Stroboscopic perturbation for treating a class of nonlinear wave equations. J. Math. Phys. **5**, 231–244 (1964)
19. Lagrange, J.L.: Recherches sur la nature et la propagation du son, *Miscellanea Philosophico-Mathematica Societatis Privatae Taurinensis I*, 2rd Pagination, i-112, 1759 (see also Œuvres, Tome 1, 39-148)
20. Lagrange J.L., *Mécanique analytique*, Paris, 1788 – 3rd Edition, Mallet-Bachelier, Gendre et successeur de Bachelier, Imprimeur-Libraire du bureau des longitudes, de l'école Polytechnique, de l'école centrale des arts et manufactures, Paris, (1853)
21. Luongo, A., Ferretti, M., Di Nino, S.: Stability and bifurcation of structures: statical and dynamical systems. Springer Nature, New York (2023)
22. Mindlin, R.D.: Second gradient of strain and surface-tension in linear elasticity. Int. J. Solids Struct. **1**, 417–438 (1965)
23. Pflüger, A.: Stabililätsprobleme der elastostatik. Springer-Verlag, Berlin (1964)
24. Rosenau, P.: Dynamics of dense lattices. Phys. Rev. B **36**(7), 5868–5876 (1987)
25. Toupin R.A. and Gazis D.C., Surface effects and initial stress in continuum and lattice models of elastic crystals. In: Wallis, R.F. (Ed.), *Proc. Int. Conf. Lattice Dynamics*, Copenhagen, Denmark, August 5-9 1963, 597-605, Pergamon Press, (1964)
26. Triantafyllidis, N., Bardenhagen, S.: On higher order gradient continuum theories in 1-D nonlinear elasticity. Derivation from and comparison to the corresponding discrete models. J. Elast. **33**, 259–293 (1993)
27. Truskinovsky, L., Vainchtein, A.: Quasicontinuum modelling of short-wave instabilities in crystal lattices. Phil. Mag. **85**(33–35), 4055–4065 (2005)